The Plant Cell, Vol. 23: 2514–2535, July 2011, www.plantcell.org

Genome-Wide Binding Site Analysis of FAR-RED ELONGATED HYPOCOTYL3 Reveals Its Novel Function in *Arabidopsis* Development [W]

Xinhao Ouyang,[a,b,c,1] Jigang Li,[a,b,1] Gang Li,[a,1] Bosheng Li,[a,1] Beibei Chen,[a] Huaishun Shen,[a] Xi Huang,[a] Xiaorong Mo,[a] Xiangyuan Wan,[d] Rongcheng Lin,[e] Shigui Li,[c] Haiyang Wang,[a,d] and Xing Wang Deng[a,b,d,2]

[a] Department of Molecular, Cellular, and Developmental Biology, Yale University, New Haven, Connecticut, 06520-8104
[b] Peking-Yale Joint Center for Plant Molecular Genetics and Agro-Biotechnology, National Laboratory of Protein Engineering and Plant Genetic Engineering, College of Life Sciences, Peking University, Beijing 100871, China
[c] Rice Research Institute of Sichuan Agriculture University, Chengdu, Sichuan 611130, China
[d] National Engineering Research Center for Crop Molecular Design, Beijing 100085, China
[e] Key Laboratory of Photobiology, Institute of Botany, Chinese Academy of Sciences, Beijing 100093, China

FAR-RED ELONGATED HYPOCOTYL3 (FHY3) and its homolog FAR-RED IMPAIRED RESPONSE1 (FAR1), two transposase-derived transcription factors, are key components in phytochrome A signaling and the circadian clock. Here, we use chromatin immunoprecipitation–based sequencing (ChIP-seq) to identify 1559 and 1009 FHY3 direct target genes in darkness (D) and far-red (FR) light conditions, respectively, in the *Arabidopsis thaliana* genome. FHY3 preferentially binds to promoters through the FHY3/FAR1 binding motif (CACGCGC). Interestingly, FHY3 also binds to two motifs in the 178-bp *Arabidopsis* centromeric repeats. Comparison between the ChIP-seq and microarray data indicates that FHY3 quickly regulates the expression of 197 and 86 genes in D and FR, respectively. FHY3 also coregulates a number of common target genes with PHYTOCHROME INTERACTING FACTOR 3-LIKE5 and ELONGATED HYPOCOTYL5. Moreover, we uncover a role for FHY3 in controlling chloroplast development by directly activating the expression of *ACCUMULATION AND REPLICATION OF CHLOROPLASTS5*, whose product is a structural component of the latter stages of chloroplast division in *Arabidopsis*. Taken together, our data suggest that FHY3 regulates multiple facets of plant development, thus providing insights into its functions beyond light and circadian pathways.

INTRODUCTION

Light is one of the most important environmental cues that control plant growth and development. As sessile organisms, higher plants have evolved a network of multiple photoreceptors, including phytochromes, cryptochromes, and phototropins, to sense changes in the ambient light environment in order to undergo adaptive growth and development. Among these photoreceptors, the red (R) and far-red (FR) sensing phytochromes (phys) are the best characterized (Neff et al., 2000). In *Arabidopsis thaliana*, phytochromes are encoded by a five-member gene family, designated *PHYA-PHYE*. Among these phytochromes, phyA is light labile, whereas phyB-phyE are light stable. phyA is the primary photoreceptor responsible for perceiving and mediating various responses to FR light; whereas phyB is the predominant phytochrome regulating responses to R light (Sharrock and Quail, 1989; Somers et al., 1991; Nagatani et al., 1993; Parks and Quail, 1993; Reed et al., 1993; Whitelam et al., 1993).

In the last two decades, great efforts have been made to extensively screen the signaling intermediates involved in phyA signaling, and several components responsible for the high-irradiance response branch of the phyA pathway have been identified, including FAR-RED ELONGATED HYPOCOTYL1 (FHY1) and its homolog FHY1-LIKE (FHL), and FHY3 and its homolog FAR-RED IMPAIRED RESPONSE1 (FAR1) (Whitelam et al., 1993; Hudson et al., 1999; Desnos et al., 2001; Wang and Deng, 2002; Zhou et al., 2005). The roles of these regulators in phyA signaling have been elucidated in recent studies. FHY1 and FHL, two small plant-specific proteins, are required for nuclear accumulation of light-activated phyA since phyA is localized only in the cytosol of *fhy1 fhl* double mutants (Hiltbrunner et al., 2005; Hiltbrunner et al., 2006). FHY3 and FAR1 are the key transcription factors directly activating the transcription of *FHY1* and *FHL* and thus indirectly control phyA nuclear accumulation and phyA responses (Lin et al., 2007, 2008).

FHY3 and *FAR1* encode two homologous proteins that share extensive sequence similarities with MURA, the transposase encoded by the *Mutator* element of maize (*Zea mays*; Hudson et al., 2003), and with the predicted transposase of the maize mobile element *Jittery* (Lisch, 2002; Xu et al., 2004), both of which are members of the *Mutator*-like element (MULE) superfamily

[1] These authors contributed equally to this work.
[2] Address correspondence to xingwang.deng@yale.edu.
The author responsible for distribution of materials integral to the findings presented in this article in accordance with the policy described in the Instructions for Authors (www.plantcell.org) is: Xing Wang Deng (xingwang.deng@yale.edu).
[W] Online version contains Web-only data.
www.plantcell.org/cgi/doi/10.1105/tpc.111.085126

(Lisch, 2002). As a novel transposase-derived transcription factor family, *FHY3* and *FAR1* genes are stably integrated into the genome and show no detectable sign of terminal inverted repeats or other transposon-like structures (Hudson et al., 2003). Phylogenetic analyses indicate that the *FHY3*/*FAR1*-related gene family evolved from one or several related MULE transposases during the evolution of angiosperms through a process termed "molecular domestication" with a concomitant loss of the ability to transpose (Feschotte and Pritham, 2007; Lin et al., 2007). However, why plants have evolved this new type of transcription factors and whether they function in other biological processes remain largely unknown.

Recently, several reports have shed light on the functional diversities and regulatory modes of these transposase-derived transcription factors. First, FHY3 was found to be involved in independently gating phytochrome signaling to the circadian clock (Allen et al., 2006). This finding has been extended by a recent report that FHY3 and FAR1 are involved in maintaining the rhythmic expression of *EARLY FLOWERING4* (*ELF4*), a key player of the central oscillator of the *Arabidopsis* circadian clock (Li et al., 2011). Second, two recent reports from our group both showed that FHY3 and FAR1 may work in concert with other cofactors to precisely regulate the expression of their target genes. In one study, ELONGATED HYPOCOTYL5 (HY5), a well-characterized bZIP transcription factor involved in promoting photomorphogenesis, was shown to physically interact with FHY3 and FAR1 and act as a repressor in regulating *FHY1* and *FHL* transcription (Li et al., 2010), while in another study, FHY3, FAR1, and HY5 were shown to work together with CIRCADIAN CLOCK ASSOCIATED1 (CCA1) and LATE ELONGATED HYPOCOTYL (LHY), two MYB-related transcription factors that are the key components of the central oscillator, to generate the rhythmic expression of *ELF4* (Li et al., 2011). Therefore, identification of more FHY3 direct target genes and elucidation of new roles of FHY3 in plant development will contribute to a better understanding of these transposase-derived transcription factors.

In this article, we used chromatin immunoprecipitation–based sequencing (ChIP-seq) analysis to identify the global FHY3 direct targets in the *Arabidopsis* genome. Our data revealed 1559 and 1009 FHY3 direct target genes in darkness (D) and FR light conditions, respectively, including the three previously reported FHY3 direct target genes *FHY1*, *FHL*, and *ELF4*. In addition, we show that FHY3 also directly binds to two motifs in the 178-bp repeats of the *Arabidopsis* centromeric regions. Moreover, we show that FHY3 plays a role in regulating chloroplast division by directly activating the expression of *ACCUMULATION AND REPLICATION OF CHLOROPLASTS5* (*ARC5*), a member of the dynamic GTPase family involved in chloroplast division (Gao et al., 2003). Thus, our genome-wide analysis of FHY3 direct target genes provides insights into the functional diversity of this transposase-derived transcription factor family in plants.

RESULTS

Genome-Wide Identification of in Vivo FHY3 Binding Sites

To determine the global in vivo binding sites of FHY3, we performed ChIP-seq analysis using *35S*:*3FLAG-FHY3-3HA* *fhy3-4* transgenic lines in which the 3FLAG-FHY3-3HA fusion proteins could largely rescue the long hypocotyl phenotype of the *fhy3-4* mutants (Li et al., 2011). The seedlings were grown in D or continuous FR light conditions for 4 d, and then chromatin fragments were prepared using monoclonal anti-FLAG antibodies. As a negative control, anti-FLAG ChIP assays were simultaneously performed using the wild-type (No-0) plants. Before constructing the ChIP DNA library for sequencing, we performed quantitative PCR (qPCR) analysis to check the quality of the precipitated DNA. As *FHY1* and *ELF4* are two well-characterized direct targets of FHY3 (Lin et al., 2007; Li et al., 2011), we examined whether the promoter fragments of *FHY1* and *ELF4* bound by FHY3 in vivo were enriched in our ChIP DNA samples. As shown in Supplemental Figure 1 online, the promoter fragments of *FHY1* and *ELF4* containing FHY3/FAR1 binding sites (FBSs) were specifically enriched in the anti-FLAG ChIP DNAs using *35S*:*3FLAG-FHY3-3HA* *fhy3-4* transgenic lines but not in those using the wild-type plants, indicating that our precipitated DNA samples were enriched for the real FHY3 binding fragments in vivo.

We then generated two DNA libraries, one for D and one for FR-grown samples, which were then subjected to ultra-high-throughput Solexa (Illumina) sequencing. A total of 5.5 and 4 million reads (35 bp per read) were obtained for the D and FR libraries, respectively, which were uniquely mapped to the *Arabidopsis* genome by adopting Model-based Analysis of ChIP-Seq (MACS) software (Zhang et al., 2008). Consequently, 2776 and 1968 uniquely assigned loci were identified by MACS from the D and FR libraries, respectively, as in vivo FHY3 binding peaks (which were called FHY3 binding sites; P value $< 10^{-5}$) in the *Arabidopsis* genome (Table 1; see Supplemental Data Sets 1 and 2 online).

A subsequent detailed analysis revealed that among all these FHY3 binding sites, 63 and 59% (i.e., 1745 and 1171 loci) were assigned to particular Arabidopsis Genome Initiative loci (from −1000 bp of the transcription start site to the 3′ untranslated region) in D and FR, respectively, whereas 37 and 41% (i.e., 1031 and 797 loci) of the binding sites in D and FR, respectively, reside in intergenic regions (Figure 1A, Table 1; see Supplemental Data Sets 1 and 2 online). Of the binding sites assigned to genes, around half of the binding sites in both D and FR conditions are located in the gene promoter regions, whereas the other half are located in genic regions, including exons, introns, 5′ untranslated regions, and 3′ untranslated regions (Figure 1A). These binding sites were assigned to a total of 1559 and 1009 genes in D and FR conditions, respectively, which are hereafter referred to as FHY3 direct target genes (Figure 1B; see Supplemental Data Sets 1 and 2 online). Comparison of the FHY3 direct target genes in the two conditions revealed that a common set of 785 genes are bound by FHY3 in both D and FR light conditions (Figure 1B); therefore a total of 1783

Table 1. Summary of FHY3 Binding Sites in the *Arabidopsis* Genome

Condition	Intergenic	Intron	Exon	5′-UTR	3′-UTR	Promoter	Total
D	1031	94	609	82	55	905	2776
FR	797	78	400	43	61	589	1968

UTR, untranslated region.

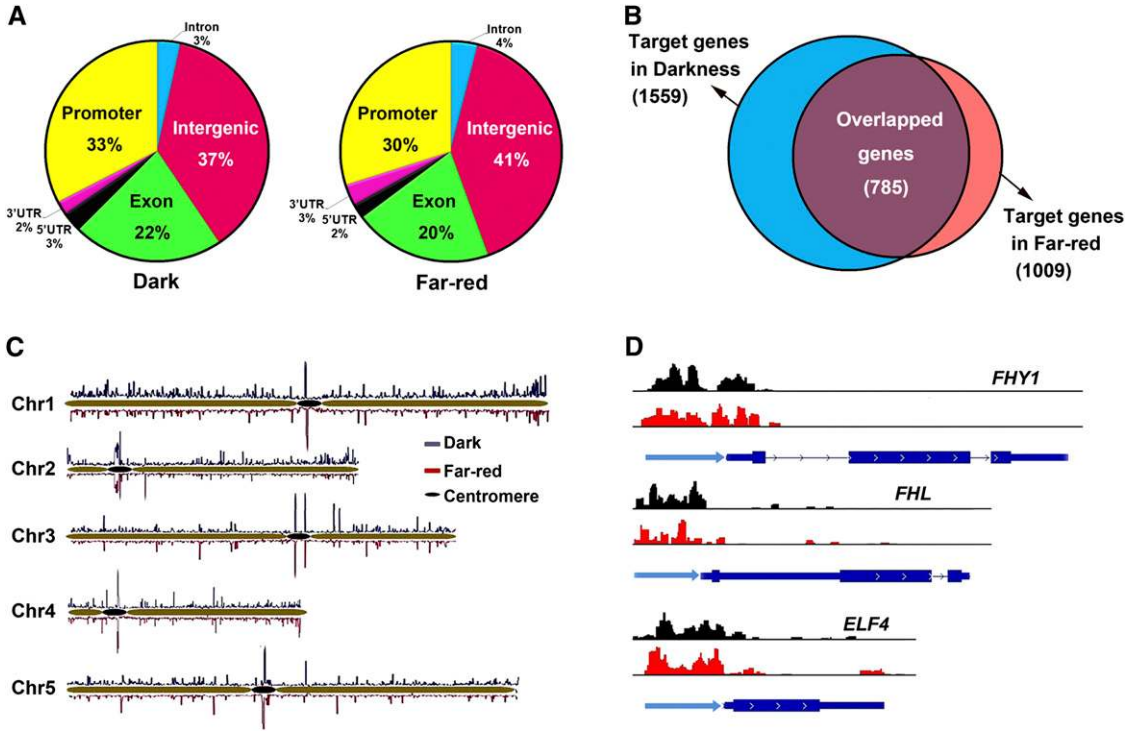

Figure 1. Overview of the FHY3 Binding Sites in the *Arabidopsis* Genome.

(A) Distribution of FHY3 binding sites in the *Arabidopsis* genome.
(B) Venn diagram showing the number and overlap of FHY3 direct target genes in D and FR light conditions.
(C) Distribution of FHY3 binding sites in the five *Arabidopsis* chromosomes. The top blue bars and the bottom red bars on each chromosome represent the positions of the FHY3 binding sites in D and FR light conditions, respectively. An oval on each chromosome indicates the location of the centromere.
(D) *FHY1*, *FHL*, and *ELF4*, three experimentally characterized FHY3 direct target genes reported in the previous studies (Lin et al., 2007; Li et al., 2011), were well identified in our genome-wide study of FHY3 direct target genes. For each gene, the mapped ChIP-seq reads in D (black) and FR (red) libraries are shown in the top and middle rows, respectively, and a schematic representation of gene structure is shown in the bottom row.

genes are identified in this study as potential FHY3 direct target genes when D and FR data are combined.

As expected, the FHY3 binding sites in both D and FR light conditions are distributed more or less evenly across the five chromosomes (Figure 1C). However, unexpectedly, the binding sites are particularly enriched in the centromeric regions (Figure 1C), which will be discussed later. We then checked the FHY3 binding profiles for *FHY1*, *FHL*, and *ELF4*, three well-documented FHY3 direct target genes in previous reports (Lin et al., 2007; Li et al., 2011). As shown in Figure 1D, FHY3 binding signals were specifically enriched in the promoter regions, but rare in the transcribed regions of these three genes in both D and FR light conditions, indicating that our analysis correctly identified the known target genes of FHY3.

Analysis of FHY3 Binding Motifs in Promoter and Genic Regions

For those FHY3 binding sites assigned to genes, we next analyzed their locations in relation to the nearby transcription start sites. Our results revealed that most of the binding sites (52 and 50% in D and FR, respectively) are located in the gene promoter regions (within 1000-bp regions upstream the transcription start sites) (Figure 2A). In the promoter regions, the locations of the FHY3 binding sites are further skewed toward regions immediately upstream of the transcription start sites, with the peak regions being at −300 to +100 bp in both D and FR light conditions (Figure 2A). This distribution pattern is consistent with the determined FHY3 binding sites in the promoters of *FHY1*, *FHL*, and *ELF4* (Lin et al., 2007; Li et al., 2011) and with the molecular function of FHY3 as a transcription factor.

Previous studies showed that FHY3 binds to a short motif, CACGCGC, termed FBS present in the promoters of *FHY1*, *FHL*, and *ELF4* (Lin et al., 2007; Li et al., 2011). Consistent with these reports, a large portion of the identified FHY3 direct target genes (57 and 49% in D and FR, respectively) contain one or more typical FBS motifs (Figure 2B). To investigate whether there is any other potential FHY3 binding motif, we used a motif-searching program, Multiple Em for Motif Elicitation (MEME) (Bailey et al., 2006), to discover statistically overrepresented motifs in the FHY3 binding regions that were assigned to genes. However, MEME failed to identify any other novel motif, and FBS was identified as the only statistically overrepresented motif in

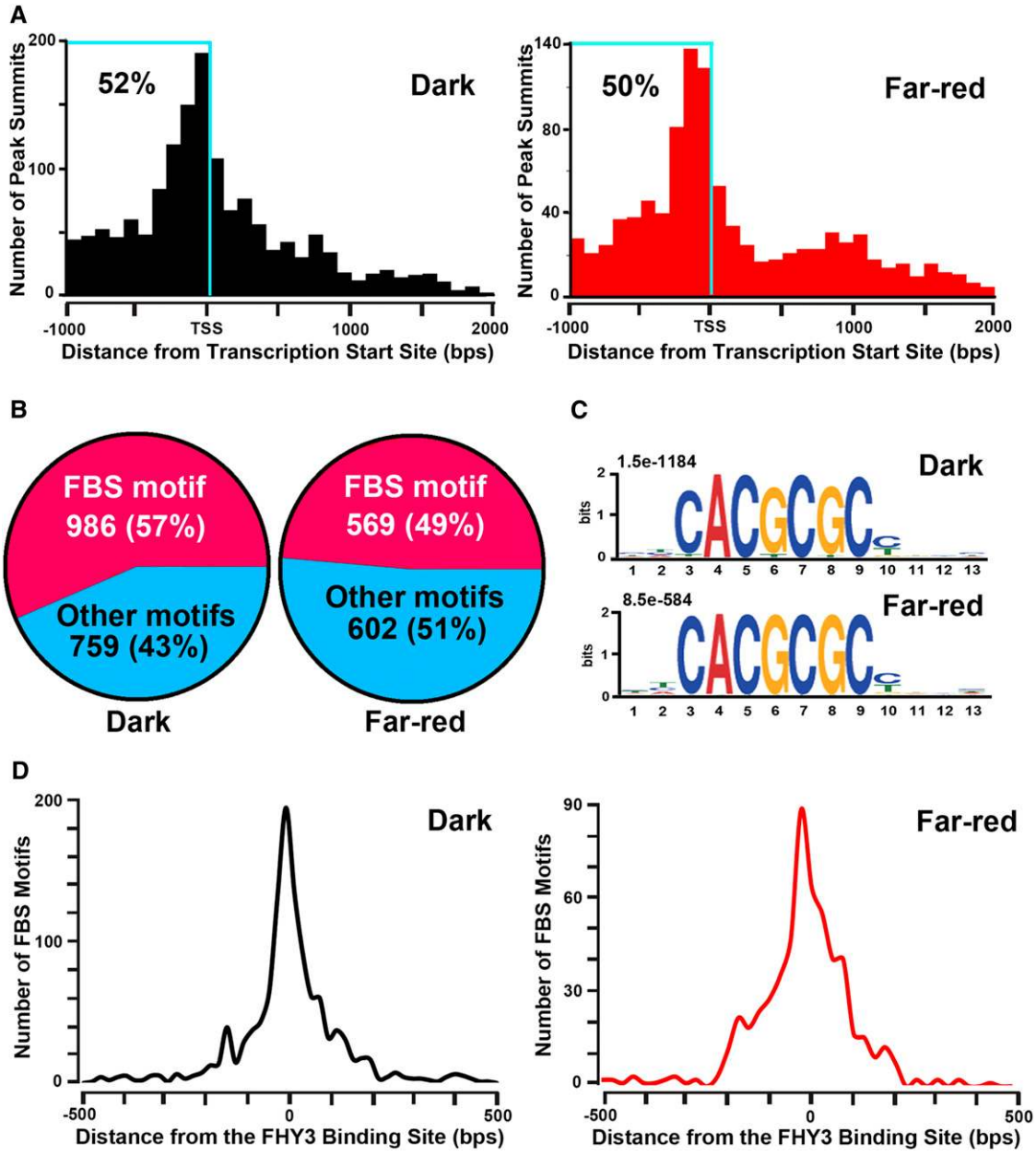

Figure 2. FHY3 Binds to the FBS Motifs in the Gene Promoters in Vivo.

(A) FHY3 binding sites are highly enriched in the −300 to +100 bp of the promoter regions in both D and FR light conditions.
(B) Percentage of FHY3 binding sites with or without FBS motifs in D and FR light conditions.
(C) Typical FBS motif (CACGCGC) was identified as the only statistically overrepresented motif in the FHY3 binding regions in D and FR light conditions by MEME software.
(D) Distribution of FBS motifs around the FHY3 binding sites (−500 to +500 bp).

these FHY3 binding regions in both D and FR light conditions (Figure 2C). As the remaining FHY3 direct target genes (43 and 51% in D and FR, respectively) do not contain any FBS, FHY3 may bind to these regions through other motifs.

Moreover, analysis of the distribution pattern of FBSs around the FHY3 binding sites (−500 to +500 bp of each predicted FHY3 binding site) revealed that the frequency of a FBS increases to reach a peak roughly at the predicted FHY3 binding sites and decreases to a background level beyond approximately −200 to +200 bp from the FHY3 binding sites in both D and FR light conditions (Figure 2D). These results indicate that the experimentally confirmed FBS may represent a major FHY3 binding motif and that FBS motifs are mainly present within −200 to +200 bp of each predicted FHY3 binding site.

Analysis of FHY3 Binding Motifs in Intergenic Regions

As mentioned above, ~40% of the FHY3 binding sites in both D and FR conditions were not assigned to specific gene loci (which were called the binding sites in intergenic regions; Figure 1A). However, an outstanding feature of this portion of FHY3 binding sites is the particular enrichment in the centromeric regions (Figure 1C). This pattern is in contrast with the previously identified genome-wide binding patterns of several transcription factors, such as HY5, BRASSINAZOLE RESISTANT1 (BZR1), and PHYTOCHROME INTERACTING FACTOR 3-LIKE5 (PIL5; also known as PHYTOCHROME INTERACTING FACTOR1 [PIF1]) (Lee et al., 2007; Oh et al., 2009). Surprisingly, based on the definitions of the centromeric regions (Copenhaver et al., 1999; Kawabe et al., 2006), more than 70% of the FHY3 binding sites in intergenic regions in both D and FR are localized in the centromeric regions of five *Arabidopsis* chromosomes (Figure 3A; see Supplemental Data Sets 1 and 2 online).

To investigate whether there are any conserved motifs in these FHY3 binding sites, MEME software was adopted again to search the sequences from −500 bp to +500 bp of the respective FHY3 binding sites in intergenic regions. Interestingly, the FBS motif observed in the gene promoter regions was not found in these binding sites. By contrast, a 12-bp consensus sequence, A[T/A]ACAC[A/T][T/A][G/A][A/C]CA, was discovered among these binding sites in both D and FR light conditions (Figure 3B). An extensive BLAST search of GenBank revealed that two stretches within the 178-bp satellite repeat of *Arabidopsis* centromeres showed exact identity to this 12-bp consensus sequence (Figure 3C) (Nagaki et al., 2003; Kawabe and Nasuda, 2005). qPCR showed that the fragment of the 178-bp centromeric repeats was specifically enriched in ChIP DNAs using *35S:3FLAG-FHY3-3HA fhy3-4* transgenic lines compared with those using the wild-type plants (see Supplemental Figure 1 online), indicating that FHY3 indeed binds to the 178-bp centromeric repeats in vivo. Electrophoretic mobility shift assays (EMSAs) showed that GST-FHY3N (glutathione *S*-transferase fused with the N-terminal DNA binding domain of FHY3), but not GST alone, bound to two wild-type probes in vitro, whereas mutating the core sequence of these motifs (CAC → aaa) effectively abolished GST-FHY3N binding to these probes (Figures 3D and 3E), indicating that FHY3 indeed binds to these two motifs in vitro. Thus, these two motifs likely represent a new type of *cis*-element that confers specific binding for FHY3 to the centromeric repeats and were therefore named FBSC-1 and -2, respectively, for FHY3 binding sites in centromeres. Notably, FBSC-1 and -2 correspond to two of the three highly conserved regions identified in the centromere tandem repeats from 41 *Arabidopsis* ecotypes (Hall et al., 2003).

We then analyzed the distribution patterns of two FBSC motifs around each putative FHY3 binding site in the centromeric regions (−500 to +500 bp of each predicted FHY3 binding site). Interestingly, both of them display a similar pattern in D and FR light, showing consecutive peaks at intervals of 178 bp (Figures 3F and 3G), consistent with the distribution pattern of the 178-bp repeats in the *Arabidopsis* centromeric regions. Consequently, FHY3 binding sites showed a consecutive tandem pattern in the centromeric regions of five *Arabidopsis* chromosomes (Figure 3H).

Determination of FHY3-Regulated Genes in D and FR by Microarray Analysis

We next sought to determine which of the FHY3 direct target genes are transcriptionally regulated by FHY3 in D and FR light conditions. We used the *FHY3p:FHY3-GR fhy3-4* transgenic lines expressing FHY3-glucocorticoid receptor (FHY3-GR) fusion proteins under the control of the *FHY3* native promoter (Lin et al., 2007), in which, without dexamethasone (DEX), the GR-fusion proteins localize in the cytoplasm, whereas, when treated with DEX, the fusion proteins translocate into the nucleus (Lloyd et al., 1994). The seedlings were grown in D or continuous FR light for 4 d and then treated with DEX or equal volume of ethanol (referred to as MOCK) and grown in the same conditions for a further 2 h before the samples were harvested. RNA samples were extracted from these samples and then hybridized with Affymetrix *Arabidopsis* ATH1 genome arrays. Four independent biological replicates for each treatment were used for the microarray analysis.

Our microarray data identified 643 and 143 differentially expressed genes in D and FR light conditions, respectively (Figure 4A; see Supplemental Data Sets 3 and 4 online), using the Significance Analysis of Microarrays method (Tusher et al., 2001) with default parameters as well as a manual setting of false discovery threshold <0.027 in D and <0.022 in FR. Notably, 197 genes in D (31% of 643 genes) and 86 genes in FR light (60% of 143 genes) contain FHY3 binding sites (Figure 4B), which were thus defined as FHY3 directly regulated genes (Table 2). Of the 197 FHY3 directly regulated genes in D, 154 (78%) and 43 (22%) genes are activated and repressed by FHY3, respectively (Figure 4B, Table 2). However, of the 86 FHY3 directly regulated genes in FR light, 85 genes (99%) are activated by FHY3, whereas only one gene, *At2g20300*, encoding a novel receptor-like kinase ALE2 (Tanaka et al., 2007), is repressed by FHY3 (Figure 4B, Table 2).

Comparison of the FHY3 directly regulated genes in two conditions revealed that FHY3 directly activates the expression of 70 genes regardless of light conditions (Figure 4B). In addition, FHY3 directly represses the expression of 43 genes in D, whereas FR light exposure released the repressive regulation of FHY3 for 42 genes (except for *At2g20300* mentioned above; Figure 4B). The constitutive activation of *FHY1* and *ELF4* and only-in-dark repression of *GA2OX6* by FHY3 were confirmed by real-time qRT-PCR analysis (see Supplemental Figure 2 online). These data suggest that the transcriptional activities of FHY3 are regulated by FR light and that FHY3 mainly acts as a transcriptional activator for most of its direct target genes, especially in FR light condition.

Moreover, 144 FHY3 directly regulated genes in D (73% of 197 genes) and 62 genes in FR light (72% of 86 genes) contain typical FBS motifs (Table 2), and most of these FBS motifs are localized in the gene promoter regions (1000 bp upstream the transcription start sites; Figure 4C), indicating that FHY3 may regulate the expression of these genes by directly binding to the FBS motifs in their gene promoters.

Gene Ontology Analysis of FHY3 Direct Target Genes

Gene Ontology (GO) analysis using the Web Gene Ontology Annotation Plot tool (Ye et al., 2006) shows that FHY3 binds to a wide

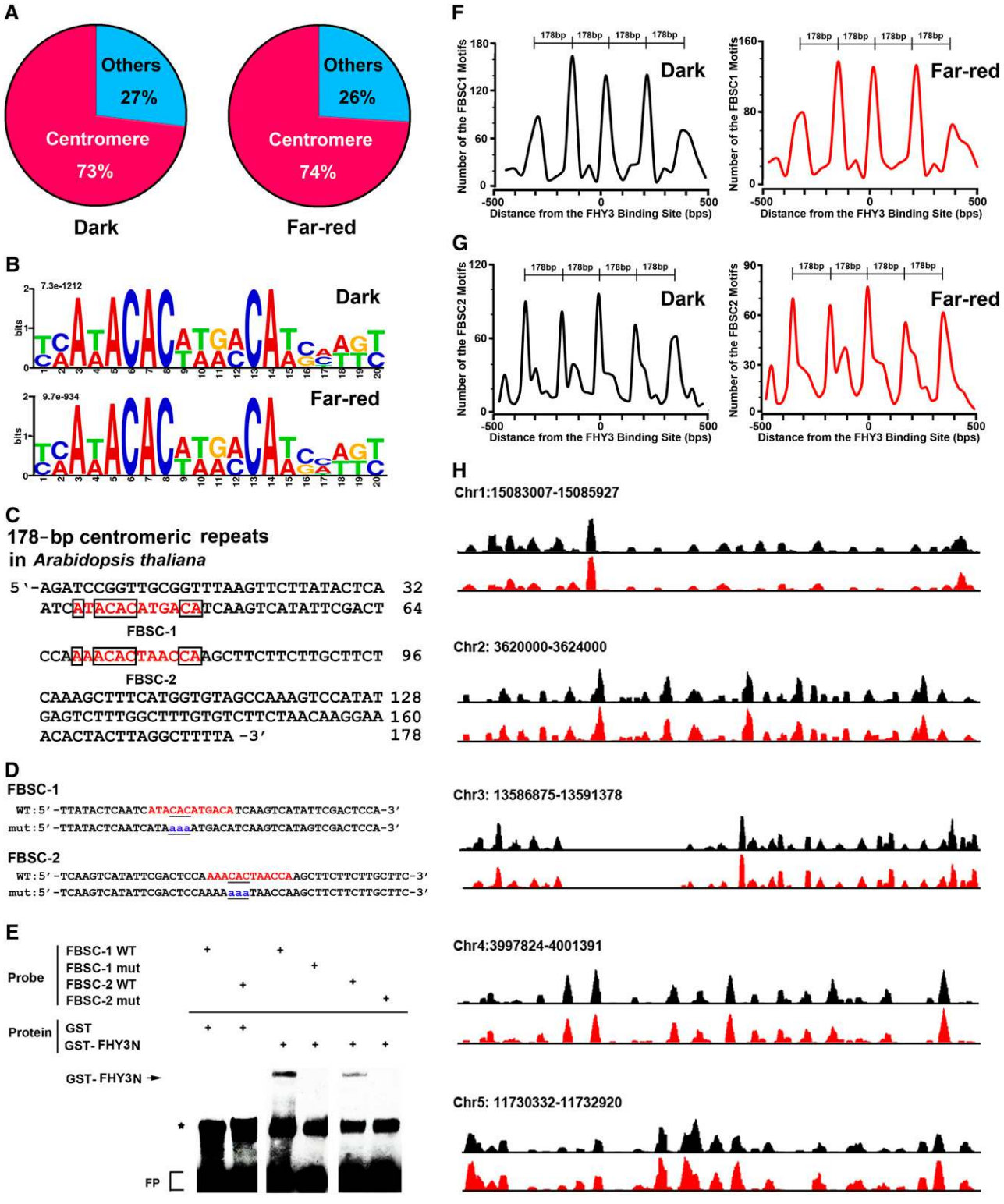

Figure 3. FHY3 Binds to Two Novel Motifs in the 178-bp Centromeric Repeats.

(A) Distribution of the FHY3 binding sites in intergenic regions in D and FR light conditions.

(B) A 12-bp consensus sequence was discovered by MEME among the FHY3 binding sites in the intergenic regions in D and FR light conditions.

(C) Two novel motifs in the 178-bp centromeric repeats in *Arabidopsis* perfectly match the 12-bp consensus sequence shown in **(B)** and were thus

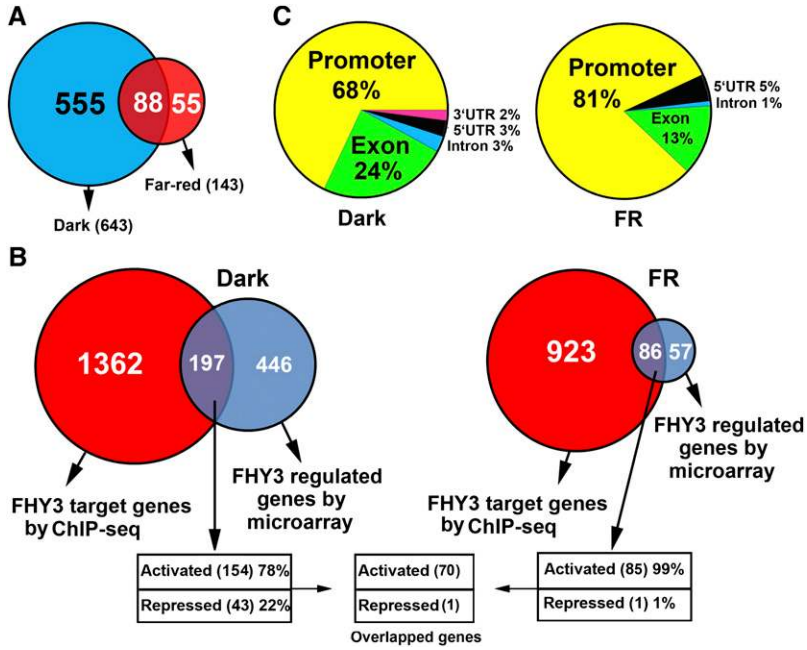

Figure 4. Identification of FHY3 Directly Regulated Genes by Comparing ChIP-seq and Microarray Data.

(A) Venn diagram showing the number of genes regulated by FHY3 in D, FR, or both conditions based on our microarray analysis.
(B) Venn diagram showing the overlaps of the FHY3 direct target genes (revealed by our ChIP-seq analysis) with FHY3 regulated genes (revealed by our microarray analysis) in D and FR light conditions.
(C) Distribution of FBS motifs in the FHY3 directly regulated genes.

range of genes involved in multiple cellular activities and biological processes (see Supplemental Figure 3 online). For example, genes involved in metabolism, development, and responses to various hormones are statistically enriched in FHY3 direct target genes compared with the whole genome (see Supplemental Figure 3 online). GO analysis was also performed to further analyze the classification of FHY3 directly regulated genes mentioned above. Interestingly, genes involved in transcription, signal transduction, biosynthesis, and development are highly enriched among these FHY3 directly regulated genes (Figure 5A). Notably, the frequency of transcription factors is ~3 times higher than that found in the whole *Arabidopsis* genome (5.9%; Riechmann et al., 2000) (Figure 5A), suggesting that they may represent early target genes of FHY3 mediating FHY3-regulated transcriptional cascades.

A large portion of FHY3 direct target genes have been studied experimentally; thus, they provide direct evidence and molecular mechanisms on how FHY3 is involved in a wide range of cellular, developmental, and regulatory processes (Figure 5B). Together with our microarray data, FHY3 was shown to directly activate (and occasionally repress) a large number of target genes with known functions in both D and FR light conditions (Figure 5B). In addition to the experimentally characterized direct target genes *FHY1*/*FHL* and *ELF4*, it is interesting to note that other key regulators in light signaling (such as *COP1*) and in the circadian clock (such as *CCA1*, *LHY*, and *CHE*) (Deng et al., 1992; Schaffer et al., 1998; Wang and Tobin, 1998; Pruneda-Paz et al., 2009) were identified as FHY3 direct target genes in our study. Direct binding of FHY3 to these genes was confirmed by ChIP-qPCR assays (see Supplemental Figure 1 online). It is also intriguing that FHY3 may directly regulate a large number of target genes involved in various hormone responses, such as abscisic acid, gibberellic acid, auxin, brassinosteroid, and ethylene, which awaits further investigation.

Figure 3. (continued).

named FBSC-1 and -2 (shown in red) for FHY3 binding sites in centromeric regions. The boxed nucleotides represent the conserved positions between these two motifs.
(D) Diagram of the wild-type and mutant (mut) centromeric fragments used as EMSA probes. Wild-type FHY3 binding sites in centromeric regions (FBSC-1 and -2) are shown in red, and substituted nucleotides in the mutant probes are shown in blue.
(E) EMSA assays showing that GST-FHY3N protein, but not GST by itself, specifically binds to the wild type (WT) but not the mutated FBSC-1 and FBSC-2 probes. Asterisk indicates nonspecific binding. FP, free probe.
(F) and **(G)** Distribution of FBSC-1 **(F)** and FBSC-2 **(G)** motifs around the FHY3 binding sites in the intergenic regions.
(H) Typical FHY3 binding loci in D (black) and FR (red) conditions in the centromeric regions of the five *Arabidopsis* chromosomes. The loci were visualized using the Integrative Genomics Viewer genome browser (Robinson et al., 2011).

Table 2. Summary of FHY3 Directly Regulated Genes

Gene ID	FBS Motif[a]	Annotation	Regulation[b]
Genes regulated by FHY3 in both D and FR			
AT1G01140	Y	CIPK9	+
AT1G01490	Y	Heavy metal–associated domain-containing protein	+
AT1G03310	Y	Isoamylase	+
AT1G08250	Y	ADT6	+
AT1G11700	Y	Unknown protein	+
AT1G17145	Y	Protein binding/zinc ion binding	+
AT1G18330	Y	EPR1	+
AT1G21640	Y	NADK2	+
AT1G22910	N	RNA recognition motif (RRM)-containing protein	+
AT1G24120	Y	ARL1	+
AT1G31930	Y	XLG3	+
AT1G35460	N	bHLH family protein	+
AT1G44170	Y	ALDH3H1	+
AT1G50660	Y	Unknown protein	+
AT1G71070	Y	Glycosyltransferase family 14 protein	+
AT1G71960	Y	ABC transporter family protein	+
AT1G72280	Y	AERO1	+
AT1G76990	Y	ACR3	+
AT1G77480	Y	Nucellin protein, putative	+
AT1G79060	Y	Unknown protein	+
AT2G20300	Y	ALE2	−
AT2G24360	N	Ser/Thr/Tyr kinase, putative	+
AT2G27820	Y	ADT6	+
AT2G28350	Y	ARF10	+
AT2G29970	Y	Heat shock protein-related	+
AT2G37678	Y	FHY1	+
AT2G32970	N	Unknown protein	+
AT2G35940	Y	NIA2	+
AT2G39130	N	Amino acid transporter family protein	+
AT2G40080	Y	ELF4	+
AT2G40950	Y	BZIP17	+
AT2G40970	Y	myb family transcription factor	+
AT2G41180	Y	sigA-binding protein-related	+
AT2G41990	Y	Unknown protein	+
AT2G42900	N	Unknown protein	+
AT2G44770	Y	Phagocytosis and cell motility protein ELMO1-related	+
AT2G45590	Y	Protein kinase family protein	+
AT2G45850	Y	DNA binding family protein	+
AT3G06500	Y	β-Fructofuranosidase	+
AT3G12550	Y	XH/XS domain-containing protein	+
AT3G13040	N	myb family transcription factor	+
AT3G18050	N	Unknown protein	+
AT3G19540	Y	Unknown protein	+
AT3G25870	Y	Unknown protein	+
AT3G50060	Y	MYB77	+
AT3G57930	Y	Unknown protein	+
AT3G58750	N	CSY2	+
AT3G60260	Y	Phagocytosis and cell motility protein ELMO1-related	+
AT3G61310	N	DNA binding family protein	+
AT3G61630	Y	CRF6	+
AT4G14500	N	Unknown protein	+
AT4G17800	N	DNA binding protein-related	+
AT4G22160	Y	Unknown protein	+
AT4G23060	Y	IQD22	+
AT4G28610	Y	PHR1	+
AT4G31170	Y	Protein kinase family protein	+
AT4G35380	Y	Guanine nucleotide exchange family protein	+

(Continued)

Table 2. (continued).

Gene ID	FBS Motif[a]	Annotation	Regulation[b]
AT4G37890	Y	EDA40	+
AT5G01780	N	Oxidoreductase	+
AT5G03530	N	RABC2A	+
AT5G10030	Y	TGA4	+
AT5G10460	N	Haloacid dehalogenase-like hydrolase family protein	+
AT5G12050	Y	Unknown protein	+
AT5G14690	Y	Unknown protein	+
AT5G15410	Y	DND1	+
AT5G19050	Y	Unknown protein	+
AT5G47640	Y	NF-YB2	+
AT5G62070	Y	IQD23	+
AT5G65430	Y	GRF8	+
AT5G67260	Y	CYCD3	+
AT5G67300	Y	MYBR1	+
Genes regulated by FHY3 only in D			
AT1G01300	Y	Aspartyl protease family protein	+
AT1G02400	Y	GA2OX6	–
AT1G03970	Y	GBF4	+
AT1G09390	Y	GDSL-motif lipase/hydrolase family protein	+
AT1G09920	Y	TRAF-type zinc finger-related	+
AT1G13020	N	Eukaryotic translation initiation factor	+
AT1G13380	Y	Unknown protein	+
AT1G15800	Y	Unknown protein	+
AT1G19480	N	HhH-GPD base excision DNA repair family protein	+
AT1G20330	Y	SMT2	+
AT1G21900	Y	emp24/gp25L/p24 family protein	+
AT1G22270	Y	Unknown protein	+
AT1G23710	Y	Unknown protein	–
AT1G23820	Y	SPDS1	+
AT1G25560	Y	TEM1	–
AT1G30690	N	SEC14 cytosolic factor family protein	–
AT1G34000	Y	OHP2	+
AT1G35140	Y	PHI-1	–
AT1G47400	N	Unknown protein	–
AT1G49450	Y	Transducin family protein	+
AT1G53170	Y	ERF8	+
AT1G55350	Y	DEK1	+
AT1G55810	N	Uracil phosphoribosyltransferase	–
AT1G59970	Y	Matrixin family protein	+
AT1G62520	Y	Unknown protein	+
AT1G62870	Y	Unknown protein	+
AT1G68790	Y	LINC3	+
AT1G69570	N	Dof-type zinc finger domain-containing protein	–
AT1G72200	Y	Zinc finger (C3HC4-type RING finger) family protein	+
AT1G77850	Y	ARF17	+
AT1G78420	Y	Protein binding/zinc ion binding	+
AT1G78610	N	MSL6	+
AT1G80440	Y	Kelch repeat-containing F-box family protein	–
AT2G01490	Y	Phytanoyl-CoA dioxygenase (PhyH) family protein	+
AT2G01910	N	ATMAP65-6	+
AT2G07698	N	ATP synthase alpha chain	–
AT2G19800	N	MIOX2	+
AT2G23170	N	GH3.3	–
AT2G27080	Y	Harpin-induced protein-related	–
AT2G34500	Y	CYP710A1	+
AT2G36220	Y	Unknown protein	–
AT2G39200	N	MLO12	–
AT2G39980	N	Transferase family protein	+

(Continued)

Table 2. (continued).

Gene ID	FBS Motif[a]	Annotation	Regulation[b]
AT2G41260	N	M17	–
AT2G41660	Y	MIZ1	+
AT2G42870	Y	PAR1	+
AT2G43000	N	anac042	–
AT2G45160	Y	Scarecrow transcription factor family protein	+
AT2G45750	N	Dehydration-responsive family protein	+
AT2G46060	Y	Transmembrane protein-related	+
AT2G46830	Y	CCA1	+
AT3G02500	Y	Unknown protein	+
AT3G02550	Y	LBD41	–
AT3G03470	Y	CYP89A9	–
AT3G06080	Y	Unknown protein	+
AT3G07580	Y	Unknown protein	+
AT3G10760	Y	myb family transcription factor	+
AT3G11900	N	ANT1	+
AT3G14850	Y	Unknown protein	+
AT3G15210	Y	ERF4	–
AT3G17860	Y	JAZ3	–
AT3G17930	Y	Unknown protein	+
AT3G27050	N	Unknown protein	+
AT3G27270	Y	Unknown protein	+
AT3G50070	Y	CYCD3;3	+
AT3G51670	N	SEC14 cytosolic factor family protein	+
AT3G51950	Y	Zinc finger (CCCH-type) family protein	+
AT3G54000	Y	Unknown protein	–
AT3G56360	Y	Unknown protein	–
AT3G56480	Y	Myosin heavy chain-related	+
AT3G60630	N	Scarecrow transcription factor family protein	+
AT3G61590	Y	HWS	+
AT3G63090	Y	Ubiquitin thiolesterase	+
AT4G00730	Y	ANL2	+
AT4G01100	N	ADNT1	+
AT4G03340	Y	Glycosyltransferase family 14 protein	+
AT4G03610	Y	Unknown protein	+
AT4G04210	Y	PUX4	+
AT4G15120	N	VQ motif-containing protein	–
AT4G16670	Y	Phosphoinositide binding	–
AT4G17100	Y	Unknown protein	+
AT4G17490	Y	ATERF6	–
AT4G21810	Y	DER2.1	+
AT4G22150	Y	PUX3	+
AT4G26740	Y	ATS1	–
AT4G27260	N	WES1	–
AT4G27280	Y	Calcium binding EF hand family protein	–
AT4G29140	Y	MATE efflux protein-related	–
AT4G30210	N	ATR2	–
AT4G31920	Y	ARR10	+
AT4G32020	Y	Unknown protein	+
AT4G33080	Y	Protein kinase, putative	+
AT4G39800	Y	MIPS1	+
AT5G01600	Y	ATFER1	+
AT5G01610	Y	Unknown protein	+
AT5G02200	Y	FHL	–
AT5G07030	Y	Aspartic-type endopeptidase	+
AT5G11090	N	Ser-rich protein-related	–
AT5G11160	Y	APT5	+
AT5G12440	Y	Nucleic acid binding/nucleotide binding/zinc ion binding	+
AT5G13300	Y	SFC	+

(Continued)

Table 2. (continued).

Gene ID	FBS Motif[a]	Annotation	Regulation[b]
AT5G17350	Y	Unknown protein	−
AT5G18830	Y	SPL7	+
AT5G19120	N	Aspartic-type endopeptidase	−
AT5G22630	Y	ADT6	+
AT5G23090	Y	NF-YB13	−
AT5G24870	N	Zinc finger (C3HC4-type RING finger) family protein	+
AT5G24930	Y	Zinc finger (B-box type) family protein	+
AT5G27420	Y	Zinc finger (C3HC4-type RING finger) family protein	−
AT5G35735	N	Auxin-responsive family protein	−
AT5G40150	N	Peroxidase, putative	+
AT5G42280	N	DC1 domain-containing protein	−
AT5G42880	N	Unknown protein	+
AT5G42950	Y	GYF domain-containing protein	+
AT5G44210	N	ERF9	+
AT5G46790	Y	Unknown protein	+
AT5G47230	Y	ERF5	−
AT5G47240	N	atnudt8	+
AT5G49080	N	Transposable element gene	+
AT5G50450	Y	Zinc finger (MYND type) family protein	+
AT5G54960	N	PDC2	−
AT5G59820	N	RHL41	−
AT5G63810	N	BGAL10	+
AT5G64660	N	U-box domain-containing protein	−
AT5G67110	Y	ALC	+
AT5G67200	Y	Leu-rich repeat transmembrane protein kinase, putative	+
Genes regulated by FHY3 only in FR			
AT1G01420	N	UGT72B3	+
AT1G48280	Y	Hyp-rich glycoprotein family protein	+
AT1G68550	N	AP2 domain-containing transcription factor, putative	+
AT2G28890	N	PLL4	+
AT3G14770	N	Nodulin MtN3 family protein	+
AT3G19720	Y	ARC5	+
AT4G14490	N	Forkhead-associated domain-containing protein	+
AT4G34200	Y	EDA9	+
AT4G36930	Y	SPT	+
AT4G36990	Y	HSF4	+
AT5G06265	N	Hyaluronan-mediated motility receptor-related	+
AT5G07240	N	IQD24	+
AT5G53570	Y	RabGAP/TBC domain-containing protein	+
AT5G62350	N	Invertase/pectin methylesterase inhibitor family protein	+
AT5G67480	Y	BT4	+

[a]The corresponding gene contains (Y) or does not contain (N) an FBS motif.
[b]+, Genes positively regulated by FHY3; −, genes negatively regulated by FHY3.

FHY3 Coregulates Some Common Target Genes with PIL5 and HY5

To investigate what other transcription factors may be involved in coregulation with FHY3, we systematically analyzed the 1-kb sequences surrounding the FHY3 binding sites (−500 to +500 bp) that were assigned to genes. We looked for enrichment of other known *cis*-elements for multiple families of transcription factors using the *Arabidopsis cis*-regulatory element database (Molina and Grotewold, 2005). This analysis revealed that in addition to the FBS motif, which is highly enriched around the FHY3 binding sites, several other *cis*-elements, including G-box, GCC-box, and ABRE, appeared at a higher frequency surrounding the FHY3 binding sites than in the whole genome (Figure 6A).

G-box is a well-known light-responsive *cis*-element that could be bound by the basic helix-loop-helix (bHLH) transcription factors (such as PIL5 and PIF3) and bZIP transcription factors (such as HY5) (Chattopadhyay et al., 1998; Oh et al., 2007, 2009; Shin et al., 2007). A recent ChIP-chip analysis identified 748 PIL5-direct target genes in *Arabidopsis* imbibed seeds (Oh et al., 2009). Comparison of these PIL5 direct target genes with FHY3 direct target genes in D revealed that a total of 136 genes may be coregulated by PIL5 and FHY3 (Figure 6B; see Supplemental Data Set 5 online). Analysis of G-box locations among these PIL5/FHY3

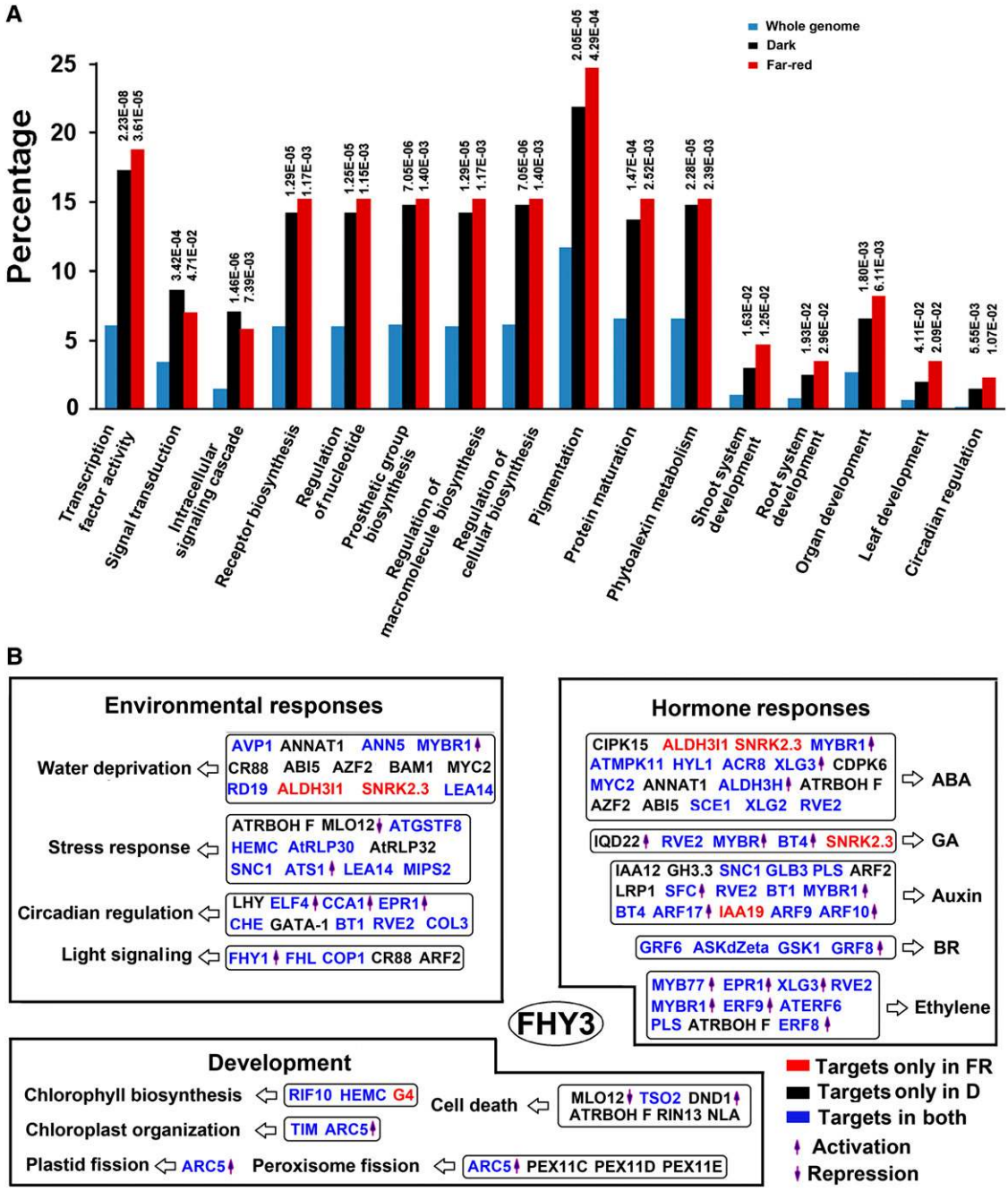

Figure 5. Functional Classification Analysis of FHY3 Direct Target Genes.

(A) Enrichment of selected GO categories in FHY3 directly regulated genes. Numbers on the top are P values (hypergeometric test) by comparing the percentage of the corresponding categories in the FHY3 directly regulated genes in D or FR light with that in the whole genome.
(B) Representative FHY3 direct target genes with known functions in various cellular processes and response/regulatory pathways. FHY3 direct target genes in D, FR, or both conditions are in black, red, or blue, respectively. Genes upregulated and downregulated by FHY3 in our microarray analyses are indicated by the directions of the arrows. ABA, abscisic acid; BR, brassinosteroid; GA, gibberellic acid.

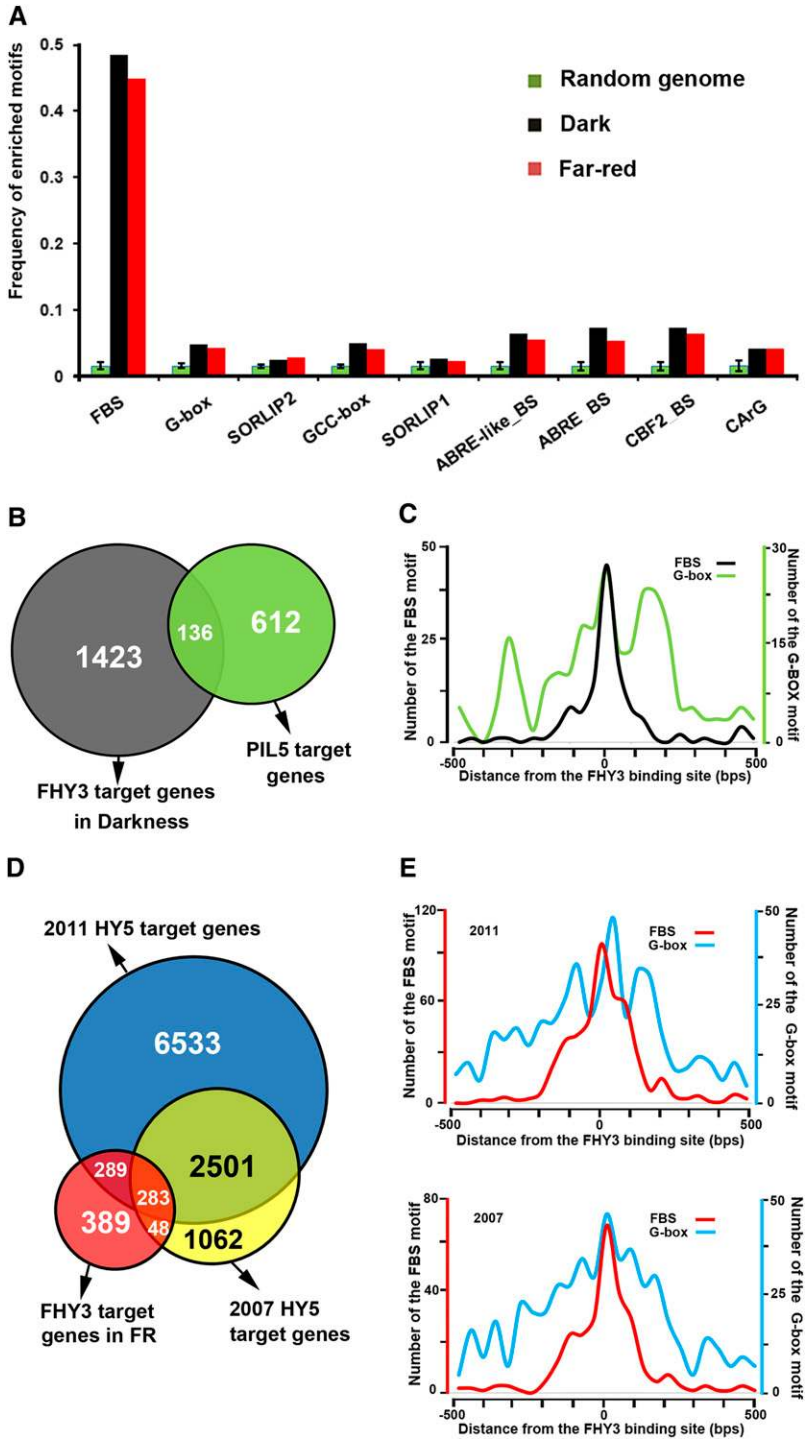

Figure 6. FHY3 Coregulates Some Common Target Genes with PIL5 and HY5.

(A) Analyses of the 1-kb sequences surrounding the FHY3 binding sites revealed enrichment of several other *cis*-elements (in addition to FBS) around the FHY3 binding sites compared with the random genome (permutation test, $P < 0.001$).

(B) Venn diagram showing the overlap of FHY3 direct target genes in D revealed in our study and PIL5 direct target genes reported in a recent study (Oh et al., 2009).

(C) Distribution of G-box and FBS motifs around the FHY3 binding sites (−500 to +500 bp) among the PIL5 and FHY3 common target genes.

(D) Venn diagram showing the overlap of FHY3 direct target genes in FR light with two sets of HY5 direct target genes reported by Lee et al. (2007) and Zhang et al. (2011).

(E) Distribution of G-box and FBS motifs around the FHY3 binding sites (−500 to +500 bp) among two sets of HY5 and FHY3 common target genes.

coregulated genes showed that G-box motifs displayed several peaks around the FBS motifs (Figure 6C).

Two recent studies using the ChIP-chip approach identified 3894 and 9606 putative HY5 direct target genes, respectively, in the *Arabidopsis* genome (Lee et al., 2007; Zhang et al., 2011). To investigate how many genes may be coregulated by FHY3 and HY5, we compared the 1009 FHY3 direct target genes identified in FR light with two sets of HY5 direct target genes identified in two previous studies. Our analysis showed that 572 and 331 genes were coregulated by HY5 and FHY3, respectively, based on two sets of HY5 target genes (Figure 6D). Notably, 283 genes were identified repeatedly in two sets of HY5/FHY3 coregulated genes, including *FHY1* and *ELF4* (Figure 6D; see Supplemental Data Set 6 online).

Interestingly, HY5 and FHY3 were reported to bind their respective *cis*-elements in close proximity (<20 bp) to each other in *FHY1*/*FHL* and *ELF4* promoters (Li et al., 2010, 2011). Therefore, we asked whether this is a general characteristic for HY5 and FHY3 to coregulate their common target genes. Analysis of two sets of HY5/FHY3 common target genes both showed that G-box motifs are preferentially positioned at the locations of, or in close proximity to (within −200 to +200 bp), FBS motifs (Figure 6E), a pattern distinct from that of the G-box locations in the PIL5/FHY3 coregulated genes (Figure 6C). Considering the fact that HY5 and FHY3 physically interact with each other (Li et al., 2010), our data suggest that HY5/FHY3 interaction and cobinding to the promoters may represent a pivotal module to regulate a large number of their common target genes.

FHY3 Is Involved in the Regulation of Chloroplast Division by Directly Activating *ARC5* Transcription

It was interesting to notice that FHY3 regulates several genes involved in chloroplast development (Figure 5B). Therefore, we examined whether the *fhy3* mutant has any defects in chloroplast development. Interestingly, microscopy observations show that leaf mesophyll cells in *fhy3-4* mutants contain fewer and larger chloroplasts than do wild-type cells (Figures 7A and 7B), whereas introduction of 3FLAG-FHY3-3HA (under the 35S constitutive promoter) or FHY3-GR (under the *FHY3* native promoter with DEX treatment) fusion proteins into the *fhy3-4* mutants rescued the chloroplast defect phenotypes (Figures 7C and 7D), indicating that FHY3 indeed regulates chloroplast development.

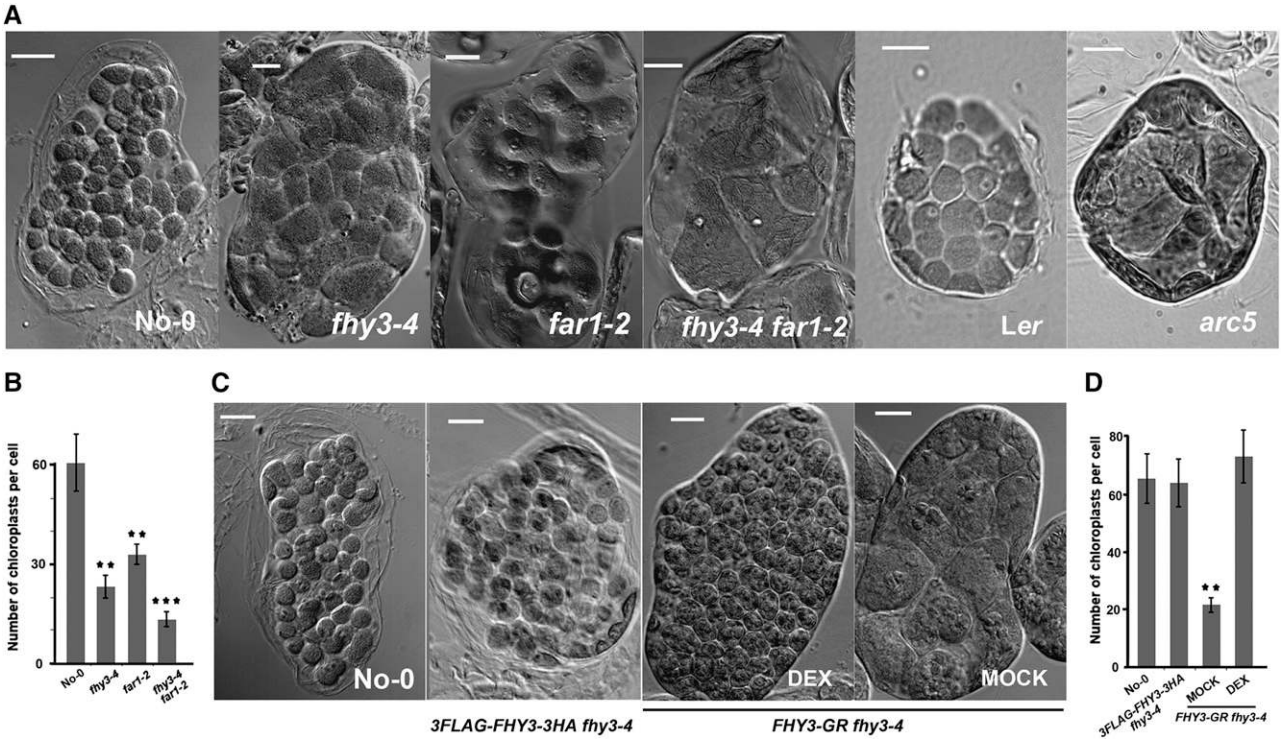

Figure 7. FHY3 and FAR1 Are Involved in the Control of Chloroplast Development.

(A) Comparison of chloroplasts in leaf mesophyll cells of 10-d-old wild-type (No-0 and Landsberg *erecta* ecotypes), *fhy3-4*, *far1-2*, *fhy3-4 far1-2*, and *arc5* mutant plants grown in continuous white light conditions. Bar = 10 μm.

(B) Chloroplast numbers are significantly decreased in the leaf mesophyll cells of *fhy3-4*, *far1-2*, and *fhy3-4 far1-2* mutants compared with the wild-type plants. More than 20 leaf mesophyll cells were counted for each plant. Student's *t* tests were performed to calculate the statistical significance (**P < 0.01 and ***P < 0.001). Error bars represent SD.

(C) and **(D)** Transgenic expression of FHY3-GR (under the *FHY3* native promoter with DEX treatment) or 3FLAG-FHY3-3HA (under the 35S promoter) sufficiently rescued the chloroplast shape **(C)** and number **(D)** phenotypes of the *fhy3-4* mutants. **P < 0.01 by Student's *t* test. Error bars represent SD.

In addition, chloroplast number was also reduced in the *far1-2* mutants and was much further reduced in the *fhy3-4 far1-2* double mutants compared with that in the wild-type plants (Figures 7A and 7B), indicating that FHY3 and FAR1 act together in the control of chloroplast development, although FAR1 plays a less predominant role compared with FHY3.

The phenotypes of *fhy3*, *far1*, and *fhy3 far1* mutants are reminiscent of what was observed in the loss-of-function mutant of *ARC5*, encoding a cytosolic dynamin-like protein involved in the latter stages of chloroplast division in *Arabidopsis* (Figure 7A; Robertson et al., 1996; Gao et al., 2003; Yun and Kawagoe, 2009). Interestingly, *ARC5* was identified as a FHY3 direct target gene in our study (Figure 5B), and FHY3 specifically binds to the promoter region of *ARC5* in both D and FR light conditions (Figure 8A; see Supplemental Figure 1 online). To further confirm whether FHY3 (and possibly FAR1) bind to the *ARC5* promoter through the only FBS motif located at approximately −65 bp upstream of the ATG start codon, we performed yeast one-hybrid assays, in which the wild-type and FBS-mutated *ARC5* promoter fragments were used to drive *LacZ* reporter gene expression (Figure 8B). Our results showed that AD-FHY3 and AD-FAR1 bind to the wild type, but not the FBS-mutated *ARC5* promoter fragments (Figure 8C), confirming that the typical FBS motif in the *ARC5* promoter mediates the binding of FHY3 and FAR1 to the promoter.

Next, we asked whether the *ARC5* transcript level is regulated by FHY3 and FAR1. Real-time qRT-PCR showed that the transcript levels of *ARC5*, but not those of *ARC3* and *ARC6*, two other genes also involved in controlling chloroplast division (Marrison et al., 1999; Holzinger et al., 2008) but not identified as FHY3 target genes in our study, were severely attenuated in the *fhy3*, *far1*, and *fhy3 far1* mutants (Figure 9A). However, *ARC5* expression was efficiently restored in the *35S:3FLAG-FHY3-3HA fhy3-4* transgenic lines in which 3FLAG-FHY3-3HA fusion proteins were expressed at high levels (Figure 9B; Li et al., 2011). This restoration was further confirmed by examination of *ARC5* transcript levels in the *FHY3p:FHY3-GR fhy3-4* transgenic seedlings with MOCK or DEX treatment (Figure 9C). Moreover, detailed time-course qPCRs using this transgenic line showed that in both D and FR light conditions, the *ARC5* transcript levels were induced rapidly after the DEX, but not the MOCK treatment within 2 h, indicating that FHY3 indeed directly activates *ARC5* transcription (Figure 9D).

Finally, we examined whether restoration of *ARC5* in the *fhy3-4* mutant could rescue its chloroplast defects by transforming the *35S:FLAG-ARC5* construct into the *fhy3-4* mutants. Analysis of the transgenic plants showed that reintroduction of FLAG-ARC5 under the 35S promoter could rescue the chloroplast defects of the *fhy3-4* mutant (Figures 10A to 10D). By contrast, ARC5-GFP (green fluorescent protein) fusion proteins under the control of the native *ARC5* promoter in the *fhy3-4* mutant were not expressed and thus could not rescue its chloroplast defects (Figures 10E and 10F), further confirming that *ARC5* is indeed a FHY3 direct target gene in *Arabidopsis*. Taken together, our data demonstrate that FHY3 controls chloroplast division by directly activating *ARC5* transcription.

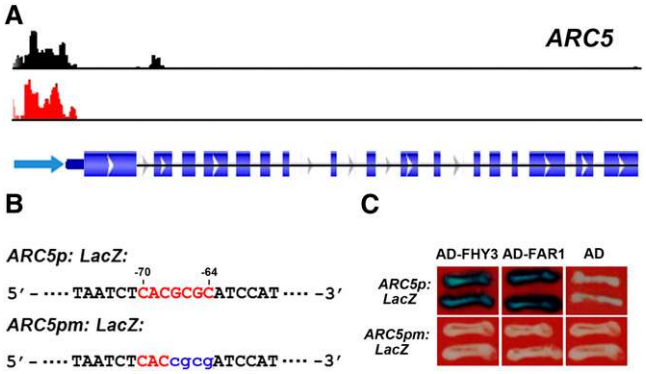

Figure 8. FHY3 Directly Binds to the *ARC5* Gene Promoter.

(A) *ARC5* was identified as a FHY3 direct target gene in both D and FR light conditions. The mapped ChIP-seq reads in D (black) and FR (red) libraries are shown in the top and middle rows, respectively, and a schematic representation of *ARC5* gene structure is shown in the bottom row.

(B) Diagram of the wild-type and mutant (m) *ARC5* promoter fragments used to drive *LacZ* reporter gene expression in yeast one-hybrid assays. The adenine residue of the translational start codon (ATG) was assigned position +1, and the numbers above the nucleotide sequence were counted based on this number. FBS motifs are shown in red, and nucleotide substitutions in the mutant fragment are shown in blue.

(C) Yeast one-hybrid assays showing that FHY3 and FAR directly bind to the wild type but not the FBS-mutated *ARC5* promoter fragment.

DISCUSSION

Several studies have been reported in recent years profiling genome-wide direct target genes for pivotal plant transcription factors, such as HY5, PIL5, AGAMOUS-LIKE15, and BZR1 (Lee et al., 2007; Oh et al., 2009; Zheng et al., 2009; Sun et al., 2010; Zhang et al., 2011). However, most of these studies were conducted using ChIP-chip, which tends to have low resolution and is often quite noisy in higher organisms (Johnson et al., 2008). In this study, we adopted a newer technique, ChIP-seq, which may effectively surmount the shortcomings of ChIP-chip (Valouev et al., 2008), to identify genome-wide direct target genes of FHY3, another important transcription factor in *Arabidopsis*.

Genome-Wide Analysis of FHY3 Direct Target Genes

FHY3 and its homolog FAR1 belong to a recently identified transcription factor family, which has been reported to play pivotal roles in phyA signaling and the circadian clock (Whitelam et al., 1993; Hudson et al., 1999; Wang and Deng, 2002; Allen et al., 2006; Lin et al., 2007; Li et al., 2011). Their protein sizes are large (~92 kD), and both of them contain transposase-like domains in the middle of their proteins and were thus proposed to originate from *Mutator*-like transposases during evolution (Lin et al., 2007). However, whether these transposase-derived transcription factors are also involved in other biological processes in plants remains largely unknown.

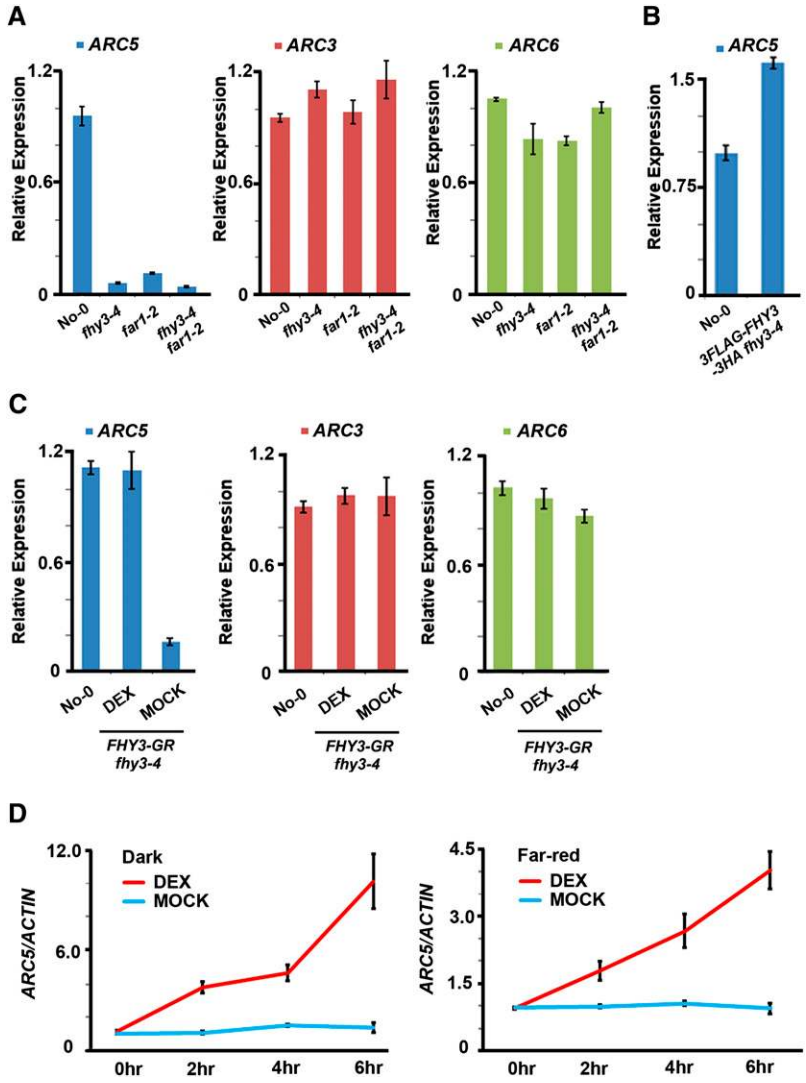

Figure 9. FHY3 Directly Activates *ARC5* Transcription.

(A) Real-time qRT-PCR analysis showing that the transcript levels of *ARC5*, but not *ARC3* or *ARC6*, were severely attenuated in the 10-d-old continuous white light–grown *fhy3-4*, *far1-2*, and *fhy3-4 far1-2* mutants compared with the wild-type plants. Error bars represent SD of triplicate experiments.
(B) Real-time qRT-PCR analysis showing that *ARC5* transcript level was restored in 10-d-old continuous white light–grown *35S:3FLAG-FHY3-3HA fhy3-4* transgenic plants.
(C) The expression of *ARC5* is upregulated by DEX but not MOCK treatment in the *FHY3p:FHY3-GR fhy3-4* plants. The expression of *ARC3* or *ARC6* is not affected by either treatment and served as the negative controls. The wild-type and *FHY3p:FHY3-GR fhy3-4* plants were grown under continuous white light for 10 d on the growth medium containing 10 μM DEX or MOCK treatment (equal volume of ethanol added to the medium) before analysis. Error bars represent SD of triplicate experiments.
(D) *ARC5* transcript levels were rapidly induced by DEX but not MOCK treatment in *FHY3p:FHY3-GR fhy3-4* transgenic plants in both D and FR light conditions. The seedlings were grown in D or FR light conditions for 4 d and then subjected to the indicated treatments and returned to the same conditions for various time periods. Error bars represent SD of triplicate experiments.

FHY3 was shown to associate with phyA in vivo and protect phyA from being recognized by the COP1/SPA protein degradation machinery (Saijo et al., 2008), suggesting that FHY3 may play additional roles in phyA signaling except for activating *FHY1/FHL* expression, and that its transcriptional activities may be regulated by phyA. In this study, we performed genome-wide analyses to identify global FHY3 direct target genes by ChIP-seq approach and FHY3 regulated genes by microarray analysis. We conducted these analyses in D (phyA plays no role) and FR light (phyA dominates) conditions, to investigate whether the binding and transcriptional regulation activities of FHY3 are regulated by FR light. Several interesting observations were made in our analyses. First, our data clearly showed that FHY3 binds to a large number of genes specifically in D or FR light conditions,

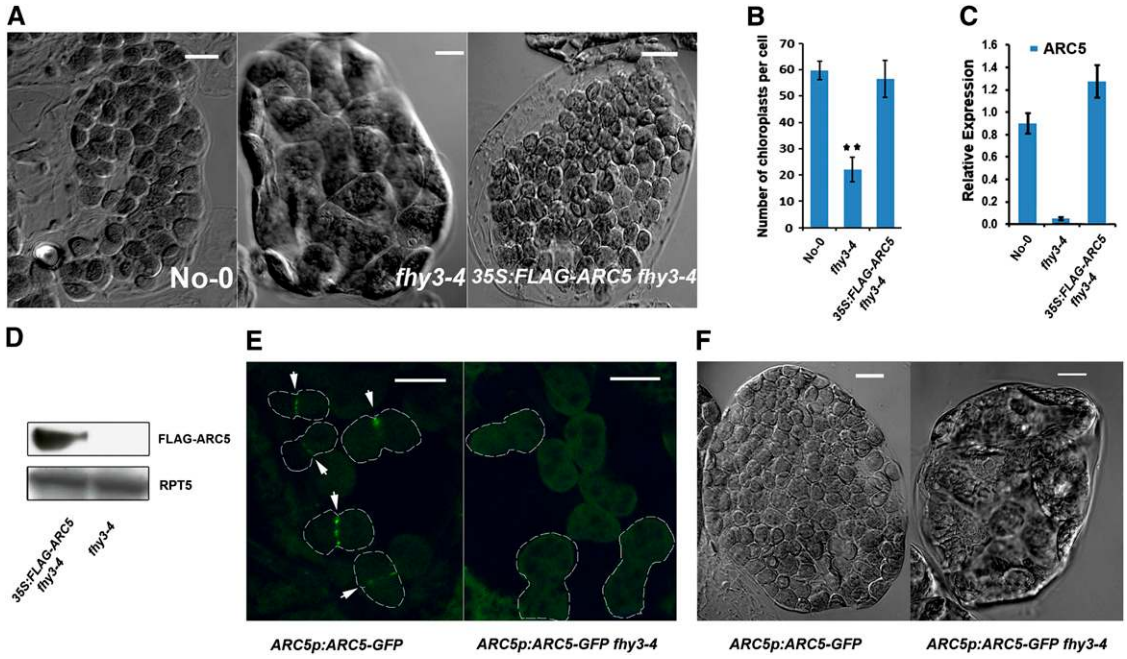

Figure 10. Overexpression of *ARC5* Rescues the Abnormal Chloroplast Phenotypes of the *fhy3* Mutants.

(A) and **(B)** Overexpression of *ARC5* rescues the phenotypes of chloroplast shape **(A)** and number **(B)** of the *fhy3-4* mutants. The plants were grown in continuous WL for 10 d before analysis. Bar = 10 μm in **(A)**. Error bars in **(B)** represent SD.

(C) *ARC5* is overexpressed in the 10-d-old continuous white light–grown *35S:FLAG-ARC5 fhy3-4* transgenic plants. Error bars represent SD of triplicate experiments.

(D) Immunoblots showing that FLAG-ARC5 fusion proteins were expressed in the 10-d-old continuous white light–grown *35S:FLAG-ARC5 fhy3-4* transgenic plants.

(E) GFP-ARC5 fusion proteins driven by the *ARC5* native promoter were expressed in the wild type but not in *fhy3-4* mutant plants. Note that GFP-ARC5 is localized to the constriction sites of dividing chloroplasts (indicated by arrows) as reported previously (Gao et al., 2003). Bar = 10 μm.

(F) Chloroplast phenotypes of *ARC5p:ARC5-GFP* and *ARC5p:ARC5-GFP fhy3-4* plants grown in continuous WL for 10 d. Bar = 10 μm.

respectively (Figure 1B), demonstrating that the binding activities of FHY3 are differently regulated by FR light at least for some target genes. Second, as shown in Figure 4B, the transcriptional regulation activities of FHY3 are also regulated by FR light. An interesting observation is that FHY3 directly represses the expression of 43 genes in D; however, in FR light, the repressive regulation of FHY3 was released for 42 genes (Figure 4B). Finally, it is interesting to notice that FHY3 binds to and regulates the expression of more genes in D than in FR (Figures 1B and 4A). Next, it will be intriguing to investigate how FR light regulates the transcriptional activities of FHY3 (e.g., phyA directly modifies the activities of FHY3 or via other mechanisms not yet identified).

In addition, microarray and GO analyses indicate that FHY3 directly regulates a wide range of genes involved in various developmental processes in plants (Figures 4 and 5). This notion was further supported by the discovery that FHY3 is indeed involved in the control of chloroplast division by activating *ARC5* transcription (Figures 7 to 10). Therefore, our genome-wide analysis of FHY3 direct target genes has led to the discovery of novel functions of FHY3 that may be overlooked by traditional genetic or biochemical approaches.

Regulatory Modes of FHY3

A recent study from our group revealed how FHY3 and FAR1 function with their coregulator HY5 to fine-tune the expression of *FHY1* and *FHL*. FHY3 and FAR1 act as the transcriptional activator for *FHY1*/*FHL* expression (Lin et al., 2007), whereas HY5 acts as a repressor of *FHY1*/*FHL* expression by modulating the transcriptional activities of FHY3 and FAR1 (Li et al., 2010). This is achieved by two distinct mechanisms. The first mechanism involves steric hindrance as the *cis*-elements of HY5 and FHY3/FAR1 in the *FHY1*/*FHL* promoters are very close to each other (<10 bp away; Li et al., 2010). The second mechanism is called "sequestration" through the physical interactions between HY5 and FHY3/FAR1 (Li et al., 2010). This mechanism was also used in the regulation of some plant bHLH transcription factors (de Lucas et al., 2008; Feng et al., 2008; Hornitschek et al., 2009). However, in another report from our group, both FHY3/FAR1 and HY5 were shown to be transcriptional activators for *ELF4* expression, and in this case, their respective *cis*-elements are around 20 bp away in the *ELF4* promoter (Li et al., 2011). These interesting observations reflect the complexity of regulatory modes of even same combination of transcription factors on different target gene promoters.

Notably, this study identified a large number of common target genes that may be coregulated by FHY3 and HY5. Most of these genes, especially the 283 genes repeatedly identified in two sets of HY5 target genes, are of high confidence as they always include the well-characterized FHY3/HY5 common target genes *FHY1* and *ELF4* (Figure 6D). Analysis of G-box locations showed that G-box motifs are preferentially located in close proximity to the FBS motifs in these common target genes (Figure 6E), consistent with their locations in the *FHY1*/*FHL* and *ELF4* promoters. Thus, for these newly identified FHY3/HY5 common target genes, HY5 and FHY3 might bind to their promoters via their respective *cis*-elements, which are close to each other. They may modulate the transcriptional activities of each other through their physical interactions or through some other mechanisms, such as steric hindrance. However, more detailed molecular and biochemical studies on more specific target gene promoters need to be conducted in future studies so as to demonstrate how FHY3/FAR1 and HY5 work in concert with each other on their target gene promoters, especially to understand how their roles in gene expression are determined by the relative locations of their *cis*-elements.

At the same time, it should be noted that other types of transcription factors may be recruited to work together with FHY3 to coregulate the expression of some common target genes. This idea is supported by the fact that several other types of *cis*-elements are significantly enriched around the FHY3 binding sites (Figure 6A) and by our recent report that CCA1 and LHY, two key transcription factors in the central oscillator of the *Arabidopsis* circadian clock, also bind to the *ELF4* promoter through evening elements located ~100 bp away from the FBS motifs (Li et al., 2011). Comparison of the FHY3 direct target genes with the recently reported PIL5 direct targets revealed a total of 136 genes coregulated by FHY3 and PIL5 (Figure 6B). However, G-box locations in these genes showed a different pattern from those in the FHY3/HY5 common target genes (Figures 6C and 6E), suggesting that the coregulation mechanisms of FHY3/PIL5 may be different from those of FHY3/HY5. Thus, it is necessary to investigate whether FHY3 also physically interacts with PIL5, which may partially account for the different pattern of their binding site localizations.

FHY3 Binds to Two Novel Motifs Present in the 178-bp Centromeric Repeats

One unexpected finding of this study is that most of the FHY3 binding sites in the intergenic regions reside in centromeric regions (Figure 3A). Further analysis revealed that FHY3 directly binds to two motifs present in the 178-bp centromeric repeats (Figures 3C to 3E). To our knowledge, this feature is unique to FHY3, as it was not observed in other genome-wide binding site studies of plant transcription factors, such as HY5, PIL5, and BZR1 (Lee et al., 2007; Oh et al., 2009; Sun et al., 2010; Zhang et al., 2011). It is also interesting to notice that these two motifs are highly conserved in the centromeric tandem repeat sequences of 41 *Arabidopsis* ecotypes (Hall et al., 2003). As the 178-bp repeats are the dominant sequence elements of *Arabidopsis* centromeres and centromeric regions govern the transmission of nuclear chromosomes to the next generation of cells (Houben and Schubert, 2003; Nagaki et al., 2003), it will be interesting to investigate the biological significance of FHY3 binding to the centromeric regions in future studies.

Our data, together with those in the previous reports, indicate that FHY3 could bind to at least three various *cis*-elements (i.e., FBS, FBSC-1, and FBSC-2) in the *Arabidopsis* genome. Interestingly, all of these motifs share the CAC core sequence. This finding may facilitate the identification of novel FHY3 direct target genes in future studies, as around half of the FHY3 direct target genes do not contain any typical FBS motifs (Figure 2B).

FHY3 Plays a Role in the Control of Chloroplast Development

Chloroplasts are essential for photosynthesis, and light is a major environmental factor determining the biogenesis of chloroplasts (Pogson and Albrecht, 2011). Phytochrome-interacting transcription factors PIFs were shown to be negative regulators of chloroplast development that act by repressing the expression of genes involved in chlorophyll biosynthesis and photosynthesis (Huq et al., 2004; Shin et al., 2009; Stephenson et al., 2009). In this study, we show that FHY3, another transcription factor acting in the phytochrome signaling pathway, also plays a role in chloroplast development. However, in contrast with the roles of PIFs in repressing chlorophyll biosynthesis, FHY3 controls chloroplast division by directly activating *ARC5* transcription. Recently, *ARC5* was also shown to mediate peroxisome division (Zhang and Hu, 2010); thus, it will be interesting to investigate whether FHY3 is involved in peroxisome division as well. Moreover, as mentioned above, FHY3 associates with phyA in vivo (Saijo et al., 2008); thus, FHY3 may represent another pathway mediating phytochrome-regulated chloroplast development in *Arabidopsis*.

In summary, our genome-wide identification of FHY3 direct target genes may serve as a new starting point to systematically study the functions of FHY3. Discovery of new roles of FHY3 in plant development and elucidation of more regulatory modes of FHY3 may help in understanding the functional conservation and divergence of these transposase-derived transcription factors during evolution.

METHODS

Plant Materials and Growth Conditions

The wild-type *Arabidopsis thaliana* used in this study is of the No-0 ecotype, unless otherwise indicated. The *arc5* mutant (Gao et al., 2003) is of the Landsberg *erecta* ecotype, *ARC5p:ARC5-GFP* (Gao et al., 2003) is of the Columbia ecotype, and the *fhy3-4* (Wang and Deng, 2002), *far1-2* (Hudson et al., 1999), and *fhy3-4 far1-2* (Lin et al., 2007) mutants and *FHY3p:FHY3-GR fhy3-4* (Lin et al., 2007) and *35S:3FLAG-FHY3-3HA fhy3-4* (Li et al., 2011) transgenic plants are of the No-0 ecotype and have been described previously. The *ARC5p:ARC5-GFP fhy3-4* plants were constructed by crossing *ARC5p:ARC5-GFP* and *fhy3-4* mutant plants. The growth conditions and light sources were as described previously (Shen et al., 2005).

ChIP-seq

The homozygous *35S:3FLAG-FHY3-3HA fhy3-4* (Li et al., 2011) seedlings grown in D or continuous FR light for 4 d were used for ChIP assays

following the procedure described previously (Lee et al., 2007). Briefly, 5 g of seedlings were first cross-linked with 1% formaldehyde under vacuum, and then the samples were ground to powder in liquid nitrogen. The chromatin complexes were isolated and sonicated and then incubated with monoclonal anti-FLAG antibodies (Sigma-Aldrich). The precipitated DNA was recovered and used to generate Illumina sequencing libraries according to the manufacturer's instructions. Sequencing was conducted by Keck DNA sequencing laboratory located at Yale School of Medicine.

ChIP-seq Data Analysis

Sequencing reads from D and FR libraries were mapped to TAIR9 genome release of *Arabidopsis* using MAQ software (Li et al., 2008; He et al., 2010), allowing for up to two mismatching nucleotides and no gaps. Only uniquely mapped reads were retained for further analyses. The output of the analysis pipeline was converted to browser extensible data files for viewing the data in the Integrative Genomics Viewer genome browser (Robinson et al., 2011).

Numerous peak detection algorithms have been proposed recently for analyzing the ChIP-seq data sets, and they provide more or less similar results (Laajala et al., 2009). In this study, MACS software (Zhang et al., 2008) with default parameters (bandwidth, 300 bp; mfold, 32; P value of 1.00e-05) was used to call peaks representing enriched binding sites as described previously (Wang et al., 2009; He et al., 2010). All binding peaks were sorted based on the following criteria: (1) if a binding site resides in the gene body region, it will be further categorized according to its location in the gene body (i.e., 5′-untranslated region, exon, intron, or 3′-untranslated region); (2) if a binding site is localized in the 1000-bp region upstream of the transcription start site of a gene, it is classified as a binding site in the promoter region in our study; (3) if a binding site is assigned to more than one gene by criterion (1) or (2), then it is regarded as a binding site to each of these genes; and (4) the binding sites not selected by the above three criteria were defined as the binding sites in the intergenic regions.

Microarray Analysis

For microarray analysis, *FHY3p:FHY3-GR fhy3-4* transgenic seedlings (Lin et al., 2007) grown in D or continuous FR light for 4 d were treated with 10 μM DEX or MOCK (equal volume of ethanol) for 2 h, and then total RNA was isolated using the RNeasy plant mini kit (Qiagen). RNA quality was assessed with an Agilent 2100 Bioanalyzer, and hybridization to the Affymetrix GeneChip *Arabidopsis* ATH1 Genome Arrays was performed according to the manufacturer's instructions. Four independent biological replicates for each treatment were used for microarray analysis. Raw microarray data were normalized using the robust multiarray analysis algorithm (Irizarry et al., 2003) in the BIOCONDUCTOR affy package (http://www.bioconductor.org/packages/2.0/bioc/html/affy.html). Then the microarray data were analyzed using the Significance Analysis of Microarrays method (Tusher et al., 2001) with default parameters as well as a manual setting of false discovery threshold <0.027 in D and <0.022 in FR.

Motif Search and Gene Ontology Analysis

The 1-kb sequences (500 bp upstream and 500 bp downstream) surrounding the FHY3 binding peaks were extracted and then searched for perfect matches to the consensus transcription factor binding motifs using a Perl script. The consensus motif sequences were obtained from the AGRIS and Transfac databases (Wingender et al., 1996; Davuluri et al., 2003). The frequencies of these consensus motifs surrounding the FHY3 binding peaks were compared with those in the whole genome. Gene ontology analyses of the FHY3 direct target genes were performed using the Web Gene Ontology Annotation Plotting tool (http://wego.genomics.org.cn) (Ye et al., 2006).

Real-Time qRT-PCR

Total RNA was isolated from *Arabidopsis* seedlings using the RNeasy plant mini kit (Qiagen). cDNAs were synthesized from 2 μg total RNA using SuperScript II first-strand cDNA synthesis system (Invitrogen) according to the manufacturer's instructions. Real-time PCR was performed using the respective pair of primers and Power SYBR Green PCR Master Mix (Applied Biosystems) with a Bio-Rad CFX96 real-time PCR detection system as described previously (Li et al., 2010). PCR reactions were performed in triplicate for each sample, and the expression levels were normalized to that of an *Actin* gene. The primers used for qRT-PCR are listed in Supplemental Table 1 online.

Analysis of Chloroplast Phenotypes by Microscopy

Chloroplast size and number were observed as previously described (Osteryoung et al., 1998). Briefly, tips from expanding leaves of 10-d-old seedlings grown in continuous white light were cut and fixed with 3.5% glutaraldehyde and then incubated in 0.1 M Na_2-EDTA, pH 9.0, for 15 min at 55°C. The images were recorded with a Carl Zeiss LSM 780 microscope.

EMSA

The GST-FHY3N construct was described previously (Lin et al., 2007). EMSAs were performed using the biotin-labeled probes and the Lightshift Chemiluminescent EMSA kit (Pierce) according to the manufacturer's instructions. The sequences of the complementary oligonucleotides used to generate the biotin-labeled probes are shown in Supplemental Table 1 online.

Yeast One-Hybrid Assay

The AD-FHY3 and AD-FAR1 constructs were described previously (Wang and Deng, 2002). To generate the *ARC5p:LacZ* construct, a 191-bp wild-type promoter fragment of *ARC5* was amplified by PCR using a pair of primers (see Supplemental Table 1 online) and the genomic DNA of No-0 ecotype as templates and then cloned into the *Eco*RI-*Kpn*I sites of the pLacZi2μ vector (Lin et al., 2007). To generate the *ARC5pm:LacZ* construct in which the FBS motif (CACGCGC) was mutated to CACcgcg, the *ARC5p:LacZ* reporter plasmid was used as the template for mutagenesis reactions using the pair of primers shown in Supplemental Table 1 online and the QuikChange site-directed mutagenesis kit (Stratagene) according to the manufacturer's instructions.

Yeast one-hybrid assays were performed as described previously (Lin et al., 2007). Briefly, plasmids for AD fusions were cotransformed with the *ARC5p:LacZ* or *ARC5pm:LacZ* reporter constructs, respectively. Transformants were grown on SD/-Trp-Ura dropout plates containing X-gal (5-bromo-4-chloro-3-indolyl-β-D-galactopyranoside) for blue color development.

Immunoblotting

For immunoblots, *35S:FLAG-ARC5 fhy3-4* homozygous seedlings were homogenized in an extraction buffer containing 50 mM Tris-HCl, pH 7.5, 150 mM NaCl, 10 mM $MgCl_2$, 0.1% Tween 20, 1 mM PMSF, and 1× complete protease inhibitor cocktail (Roche). Immunoblotting was performed as described previously (Shen et al., 2005) using monoclonal anti-FLAG antibodies (Sigma-Aldrich).

Complementation Analysis

To generate the *35S:FLAG-ARC5* construct, the coding region of *ARC5* was first PCR amplified using first-strand cDNAs prepared from 10-d-old

Arabidopsis seedlings grown in continuous WL (primers shown in Supplemental Table 1 online) and then inserted into the *Kpn*I-*Sal*I sites of the pF3PZPY122 vector (Feng et al., 2003). Then, a *Bam*HI-*Eco*RI fragment containing the full-length coding sequence of FLAG-ARC5 was released and inserted into the *Bam*HI-*Eco*RI sites of the pJim19 (Kan) vector, a binary vector based on pBIN19 with *35S* promoter of *Cauliflower mosaic virus* and kanamycin resistance markers in both bacteria and plants. The *35S:FLAG-ARC5* construct was electroporated into *Agrobacterium tumefaciens* strain GV3101 and used to transform the *fhy3-4* homozygous mutants.

Accession Numbers

Sequence data from this article can be found in the Arabidopsis Genome Initiative or GenBank/EMBL databases under the following accession numbers: FHY3 (At3g22170), FAR1 (At2g15090), FHY1 (At2g37678), FHL (At5g02200), ELF4 (At2g40080), HY5 (At5g11260), PIL5/PIF1 (At2g20180), and ARC5 (At3g19720). All raw ChIP-seq data and expression profiling data have been deposited in the Gene Expression Omnibus database under accession numbers GSE30711 and GSE30712.

Supplemental Data

The following materials are available in the online version of this article.

Supplemental Figure 1. Validation of Several FHY3 Direct Target Genes and Binding Sites by ChIP-qPCR Analysis.

Supplemental Figure 2. Validation of Expression Changes of *ELF4*, *FHY1*, and *GA2OX6* in D and FR by Real-Time qRT-PCR Analysis.

Supplemental Figure 3. Functional Classification of the FHY3 Direct Target Genes.

Supplemental Table 1. Summary of Primers Used in This Study.

Supplemental Data Set 1. List of FHY3 Binding Sites in D.

Supplemental Data Set 2. List of FHY3 Binding Sites in FR Light.

Supplemental Data Set 3. List of FHY3 Regulated Genes in D.

Supplemental Data Set 4. List of FHY3 Regulated Genes in FR Light.

Supplemental Data Set 5. List of FHY3 and PIL5 Coregulated Genes.

Supplemental Data Set 6. List of FHY3 and HY5 Coregulated Genes.

ACKNOWLEDGMENTS

We thank Katherine W. Osteryoung for providing *ARC5p:ARC5-GFP* and *arc5* mutant seeds. We also thank Guangming He, Lifen Huang, Mingqiu Dai, and Shangwei Zhong for their suggestions on the project. This work was supported by the National Institutes of Health (grant GM47850 to X.W.D.) and the National Science Foundation (Awards IOS-0954313 and IOS-1026630 to H.W.). X.O. was supported by Peking-Yale Joint Center Monsanto Fellowship and a fellowship from the China Scholarship Council.

AUTHOR CONTRIBUTIONS

X.W.D., H.W., and S.L. conceived the project. X.O., G.L., and X.W.D. designed the experiments. J.L. and X.O. performed EMSA assays. J.L. and X.H. performed yeast-one hybrid assays. G.L., X.O., X.M., X.W., and R.L. generated the transgenic plants. B.L., B.C., and H.S. conducted bioinformatics analyses. X.O. performed all other experiments. J.L., X.O., and X.W.D. prepared the manuscript.

Received March 10, 2011; revised July 10, 2011; accepted July 17, 2011; published July 29, 2011.

REFERENCES

Allen, T., Koustenis, A., Theodorou, G., Somers, D.E., Kay, S.A., Whitelam, G.C., and Devlin, P.F. (2006). *Arabidopsis* FHY3 specifically gates phytochrome signaling to the circadian clock. Plant Cell **18:** 2506–2516.

Bailey, T.L., Williams, N., Misleh, C., and Li, W.W. (2006). MEME: Discovering and analyzing DNA and protein sequence motifs. Nucleic Acids Res. **34**(Web Server issue)**:** W369–W373.

Chattopadhyay, S., Ang, L.H., Puente, P., Deng, X.W., and Wei, N. (1998). *Arabidopsis* bZIP protein HY5 directly interacts with light-responsive promoters in mediating light control of gene expression. Plant Cell **10:** 673–683.

Copenhaver, G.P., et al. (1999). Genetic definition and sequence analysis of *Arabidopsis* centromeres. Science **286:** 2468–2474.

Davuluri, R.V., Sun, H., Palaniswamy, S.K., Matthews, N., Molina, C., Kurtz, M., and Grotewold, E. (2003). AGRIS: *Arabidopsis* gene regulatory information server, an information resource of *Arabidopsis* cis-regulatory elements and transcription factors. BMC Bioinformatics **4:** 25.

de Lucas, M., Davière, J.M., Rodríguez-Falcón, M., Pontin, M., Iglesias-Pedraz, J.M., Lorrain, S., Fankhauser, C., Blázquez, M.A., Titarenko, E., and Prat, S. (2008). A molecular framework for light and gibberellin control of cell elongation. Nature **451:** 480–484.

Deng, X.W., Matsui, M., Wei, N., Wagner, D., Chu, A.M., Feldmann, K.A., and Quail, P.H. (1992). *COP1*, an *Arabidopsis* regulatory gene, encodes a protein with both a zinc-binding motif and a G beta homologous domain. Cell **71:** 791–801.

Desnos, T., Puente, P., Whitelam, G.C., and Harberd, N.P. (2001). FHY1: A phytochrome A-specific signal transducer. Genes Dev. **15:** 2980–2990.

Feng, S., Ma, L., Wang, X., Xie, D., Dinesh-Kumar, S.P., Wei, N., and Deng, X.W. (2003). The COP9 signalosome interacts physically with SCF ^{COI1} and modulates jasmonate responses. Plant Cell **15:** 1083–1094.

Feng, S., et al. (2008). Coordinated regulation of *Arabidopsis thaliana* development by light and gibberellins. Nature **451:** 475–479.

Feschotte, C., and Pritham, E.J. (2007). DNA transposons and the evolution of eukaryotic genomes. Annu. Rev. Genet. **41:** 331–368.

Gao, H., Kadirjan-Kalbach, D., Froehlich, J.E., and Osteryoung, K.W. (2003). ARC5, a cytosolic dynamin-like protein from plants, is part of the chloroplast division machinery. Proc. Natl. Acad. Sci. USA **100:** 4328–4333.

Hall, S.E., Kettler, G., and Preuss, D. (2003). Centromere satellites from *Arabidopsis* populations: Maintenance of conserved and variable domains. Genome Res. **13:** 195–205.

He, G., et al. (2010). Global epigenetic and transcriptional trends among two rice subspecies and their reciprocal hybrids. Plant Cell **22:** 17–33.

Hiltbrunner, A., Tscheuschler, A., Viczián, A., Kunkel, T., Kircher, S., and Schäfer, E. (2006). FHY1 and FHL act together to mediate nuclear accumulation of the phytochrome A photoreceptor. Plant Cell Physiol. **47:** 1023–1034.

Hiltbrunner, A., Viczián, A., Bury, E., Tscheuschler, A., Kircher, S., Tóth, R., Honsberger, A., Nagy, F., Fankhauser, C., and Schäfer, E. (2005). Nuclear accumulation of the phytochrome A photoreceptor requires FHY1. Curr. Biol. **15:** 2125–2130.

Holzinger, A., Kwok, E.Y., and Hanson, M.R. (2008). Effects of *arc3*, *arc5* and *arc6* mutations on plastid morphology and stromule formation in green and nongreen tissues of *Arabidopsis thaliana*. Photochem. Photobiol. **84:** 1324–1335.

Hornitschek, P., Lorrain, S., Zoete, V., Michielin, O., and Fankhauser, C. (2009). Inhibition of the shade avoidance response by formation of non-DNA binding bHLH heterodimers. EMBO J. **28:** 3893–3902.

Houben, A., and Schubert, I. (2003). DNA and proteins of plant centromeres. Curr. Opin. Plant Biol. **6:** 554–560.

Hudson, M., Ringli, C., Boylan, M.T., and Quail, P.H. (1999). The *FAR1* locus encodes a novel nuclear protein specific to phytochrome A signaling. Genes Dev. **13:** 2017–2027.

Hudson, M.E., Lisch, D.R., and Quail, P.H. (2003). The *FHY3* and *FAR1* genes encode transposase-related proteins involved in regulation of gene expression by the phytochrome A-signaling pathway. Plant J. **34:** 453–471.

Huq, E., Al-Sady, B., Hudson, M., Kim, C., Apel, K., and Quail, P.H. (2004). Phytochrome-interacting factor 1 is a critical bHLH regulator of chlorophyll biosynthesis. Science **305:** 1937–1941.

Irizarry, R.A., Hobbs, B., Collin, F., Beazer-Barclay, Y.D., Antonellis, K.J., Scherf, U., and Speed, T.P. (2003). Exploration, normalization, and summaries of high density oligonucleotide array probe level data. Biostatistics **4:** 249–264.

Johnson, D.S., et al. (2008). Systematic evaluation of variability in ChIP-chip experiments using predefined DNA targets. Genome Res. **18:** 393–403.

Kawabe, A., Hansson, B., Hagenblad, J., Forrest, A., and Charlesworth, D. (2006). Centromere locations and associated chromosome rearrangements in *Arabidopsis lyrata* and *A. thaliana*. Genetics **173:** 1613–1619.

Kawabe, A., and Nasuda, S. (2005). Structure and genomic organization of centromeric repeats in *Arabidopsis* species. Mol. Genet. Genomics **272:** 593–602.

Laajala, T.D., Raghav, S., Tuomela, S., Lahesmaa, R., Aittokallio, T., and Elo, L.L. (2009). A practical comparison of methods for detecting transcription factor binding sites in ChIP-seq experiments. BMC Genomics **10:** 618.

Lee, J., He, K., Stolc, V., Lee, H., Figueroa, P., Gao, Y., Tongprasit, W., Zhao, H., Lee, I., and Deng, X.W. (2007). Analysis of transcription factor HY5 genomic binding sites revealed its hierarchical role in light regulation of development. Plant Cell **19:** 731–749.

Li, G., et al. (2011). Coordinated transcriptional regulation underlying the circadian clock in *Arabidopsis*. Nat. Cell Biol. **13:** 616–622.

Li, H., Ruan, J., and Durbin, R. (2008). Mapping short DNA sequencing reads and calling variants using mapping quality scores. Genome Res. **18:** 1851–1858.

Li, J., Li, G., Gao, S., Martinez, C., He, G., Zhou, Z., Huang, X., Lee, J.H., Zhang, H., Shen, Y., Wang, H., and Deng, X.W. (2010). *Arabidopsis* transcription factor ELONGATED HYPOCOTYL5 plays a role in the feedback regulation of phytochrome A signaling. Plant Cell **22:** 3634–3649.

Lin, R., Ding, L., Casola, C., Ripoll, D.R., Feschotte, C., and Wang, H. (2007). Transposase-derived transcription factors regulate light signaling in *Arabidopsis*. Science **318:** 1302–1305.

Lin, R., Teng, Y., Park, H.J., Ding, L., Black, C., Fang, P., and Wang, H. (2008). Discrete and essential roles of the multiple domains of *Arabidopsis* FHY3 in mediating phytochrome A signal transduction. Plant Physiol. **148:** 981–992.

Lisch, D. (2002). Mutator transposons. Trends Plant Sci. **7:** 498–504.

Lloyd, A.M., Schena, M., Walbot, V., and Davis, R.W. (1994). Epidermal cell fate determination in *Arabidopsis*: Patterns defined by a steroid-inducible regulator. Science **266:** 436–439.

Marrison, J.L., Rutherford, S.M., Robertson, E.J., Lister, C., Dean, C., and Leech, R.M. (1999). The distinctive roles of five different *ARC* genes in the chloroplast division process in *Arabidopsis*. Plant J. **18:** 651–662.

Molina, C., and Grotewold, E. (2005). Genome wide analysis of *Arabidopsis* core promoters. BMC Genomics **6:** 25.

Nagaki, K., Talbert, P.B., Zhong, C.X., Dawe, R.K., Henikoff, S., and Jiang, J. (2003). Chromatin immunoprecipitation reveals that the 180-bp satellite repeat is the key functional DNA element of *Arabidopsis thaliana* centromeres. Genetics **163:** 1221–1225.

Nagatani, A., Reed, J.W., and Chory, J. (1993). Isolation and initial characterization of *Arabidopsis* mutants that are deficient in phytochrome A. Plant Physiol. **102:** 269–277.

Neff, M.M., Fankhauser, C., and Chory, J. (2000). Light: An indicator of time and place. Genes Dev. **14:** 257–271.

Oh, E., Kang, H., Yamaguchi, S., Park, J., Lee, D., Kamiya, Y., and Choi, G. (2009). Genome-wide analysis of genes targeted by PHYTOCHROME INTERACTING FACTOR 3-LIKE5 during seed germination in *Arabidopsis*. Plant Cell **21:** 403–419.

Oh, E., Yamaguchi, S., Hu, J., Yusuke, J., Jung, B., Paik, I., Lee, H.S., Sun, T.P., Kamiya, Y., and Choi, G. (2007). PIL5, a phytochrome-interacting bHLH protein, regulates gibberellin responsiveness by binding directly to the *GAI* and *RGA* promoters in *Arabidopsis* seeds. Plant Cell **19:** 1192–1208.

Osteryoung, K.W., Stokes, K.D., Rutherford, S.M., Percival, A.L., and Lee, W.Y. (1998). Chloroplast division in higher plants requires members of two functionally divergent gene families with homology to bacterial *ftsZ*. Plant Cell **10:** 1991–2004.

Parks, B.M., and Quail, P.H. (1993). *hy8*, a new class of *Arabidopsis* long hypocotyl mutants deficient in functional phytochrome A. Plant Cell **5:** 39–48.

Pogson, B.J., and Albrecht, V. (2011). Genetic dissection of chloroplast biogenesis and development: An overview. Plant Physiol. **155:** 1545–1551.

Pruneda-Paz, J.L., Breton, G., Para, A., and Kay, S.A. (2009). A functional genomics approach reveals CHE as a component of the *Arabidopsis* circadian clock. Science **323:** 1481–1485.

Reed, J.W., Nagpal, P., Poole, D.S., Furuya, M., and Chory, J. (1993). Mutations in the gene for the red/far-red light receptor phytochrome B alter cell elongation and physiological responses throughout *Arabidopsis* development. Plant Cell **5:** 147–157.

Riechmann, J.L., et al. (2000). *Arabidopsis* transcription factors: Genome-wide comparative analysis among eukaryotes. Science **290:** 2105–2110.

Robertson, E.J., Rutherford, S.M., and Leech, R.M. (1996). Characterization of chloroplast division using the *Arabidopsis* mutant *arc5*. Plant Physiol. **112:** 149–159.

Robinson, J.T., Thorvaldsdóttir, H., Winckler, W., Guttman, M., Lander, E.S., Getz, G., and Mesirov, J.P. (2011). Integrative genomics viewer. Nat. Biotechnol. **29:** 24–26.

Saijo, Y., Zhu, D., Li, J., Rubio, V., Zhou, Z., Shen, Y., Hoecker, U., Wang, H., and Deng, X.W. (2008). *Arabidopsis* COP1/SPA1 complex and FHY1/FHY3 associate with distinct phosphorylated forms of phytochrome A in balancing light signaling. Mol. Cell **31:** 607–613.

Schaffer, R., Ramsay, N., Samach, A., Corden, S., Putterill, J., Carré, I.A., and Coupland, G. (1998). The *late elongated hypocotyl* mutation of *Arabidopsis* disrupts circadian rhythms and the photoperiodic control of flowering. Cell **93:** 1219–1229.

Sharrock, R.A., and Quail, P.H. (1989). Novel phytochrome sequences in *Arabidopsis thaliana*: Structure, evolution, and differential expression of a plant regulatory photoreceptor family. Genes Dev. **3:** 1745–1757.

Shen, Y., Feng, S., Ma, L., Lin, R., Qu, L.J., Chen, Z., Wang, H., and Deng, X.W. (2005). *Arabidopsis* FHY1 protein stability is regulated by light via phytochrome A and 26S proteasome. Plant Physiol. **139:** 1234–1243.

Shin, J., Kim, K., Kang, H., Zulfugarov, I.S., Bae, G., Lee, C.H., Lee, D., and Choi, G. (2009). Phytochromes promote seedling light responses by inhibiting four negatively-acting phytochrome-interacting factors. Proc. Natl. Acad. Sci. USA **106:** 7660–7665.

Shin, J., Park, E., and Choi, G. (2007). PIF3 regulates anthocyanin biosynthesis in an HY5-dependent manner with both factors directly binding anthocyanin biosynthetic gene promoters in *Arabidopsis*. Plant J. **49:** 981–994.

Somers, D.E., Sharrock, R.A., Tepperman, J.M., and Quail, P.H. (1991). The *hy3* long hypocotyl mutant of *Arabidopsis* is deficient in phytochrome B. Plant Cell **3:** 1263–1274.

Stephenson, P.G., Fankhauser, C., and Terry, M.J. (2009). PIF3 is a repressor of chloroplast development. Proc. Natl. Acad. Sci. USA **106:** 7654–7659.

Sun, Y., et al. (2010). Integration of brassinosteroid signal transduction with the transcription network for plant growth regulation in *Arabidopsis*. Dev. Cell **19:** 765–777.

Tanaka, H., Watanabe, M., Sasabe, M., Hiroe, T., Tanaka, T., Tsukaya, H., Ikezaki, M., Machida, C., and Machida, Y. (2007). Novel receptor-like kinase ALE2 controls shoot development by specifying epidermis in *Arabidopsis*. Development **134:** 1643–1652.

Tusher, V.G., Tibshirani, R., and Chu, G. (2001). Significance analysis of microarrays applied to the ionizing radiation response. Proc. Natl. Acad. Sci. USA **98:** 5116–5121.

Valouev, A., Johnson, D.S., Sundquist, A., Medina, C., Anton, E., Batzoglou, S., Myers, R.M., and Sidow, A. (2008). Genome-wide analysis of transcription factor binding sites based on ChIP-Seq data. Nat. Methods **5:** 829–834.

Wang, H., and Deng, X.W. (2002). *Arabidopsis* FHY3 defines a key phytochrome A signaling component directly interacting with its homologous partner FAR1. EMBO J. **21:** 1339–1349.

Wang, X.F., Elling, A.A., Li, X.Y., Li, N., Peng, Z.Y., He, G.M., Sun, H., Qi, Y.J., Liu, X.S., and Deng, X.W. (2009). Genome-wide and organ-specific landscapes of epigenetic modifications and their relationships to mRNA and small RNA transcriptomes in maize. Plant Cell **21:** 1053–1069.

Wang, Z.Y., and Tobin, E.M. (1998). Constitutive expression of the *CIRCADIAN CLOCK ASSOCIATED 1* (*CCA1*) gene disrupts circadian rhythms and suppresses its own expression. Cell **93:** 1207–1217.

Whitelam, G.C., Johnson, E., Peng, J.R., Carol, P., Anderson, M.L., Cowl, J.S., and Harberd, N.P. (1993). Phytochrome A null mutants of *Arabidopsis* display a wild-type phenotype in white light. Plant Cell **5:** 757–768.

Wingender, E., Dietze, P., Karas, H., and Knüppel, R. (1996). TRANSFAC: A database on transcription factors and their DNA binding sites. Nucleic Acids Res. **24:** 238–241.

Xu, Z.N., Yan, X.H., Maurais, S., Fu, H.H., O'Brien, D.G., Mottinger, J., and Dooner, H.K. (2004). *Jittery*, a *Mutator* distant relative with a paradoxical mobile behavior: Excision without reinsertion. Plant Cell **16:** 1105–1114.

Ye, J., Fang, L., Zheng, H., Zhang, Y., Chen, J., Zhang, Z., Wang, J., Li, S., Li, R., Bolund, L., and Wang, J. (2006). WEGO: A web tool for plotting GO annotations. Nucleic Acids Res. **34**(Web Server issue)**:** W293–W297.

Yun, M.S., and Kawagoe, Y. (2009). Amyloplast division progresses simultaneously at multiple sites in the endosperm of rice. Plant Cell Physiol. **50:** 1617–1626.

Zhang, H., He, H., Wang, X., Wang, X., Yang, X., Li, L., and Deng, X.W. (2011). Genome-wide mapping of the HY5-mediated gene networks in *Arabidopsis* that involve both transcriptional and post-transcriptional regulation. Plant J. **65:** 346–358.

Zhang, X., and Hu, J. (2010). The *Arabidopsis* chloroplast division protein DYNAMIN-RELATED PROTEIN5B also mediates peroxisome division. Plant Cell **22:** 431–442.

Zhang, Y., Liu, T., Meyer, C.A., Eeckhoute, J., Johnson, D.S., Bernstein, B.E., Nusbaum, C., Myers, R.M., Brown, M., Li, W., and Liu, X.S. (2008). Model-based analysis of ChIP-Seq (MACS). Genome Biol. **9:** R137.

Zheng, Y., Ren, N., Wang, H., Stromberg, A.J., and Perry, S.E. (2009). Global identification of targets of the *Arabidopsis* MADS domain protein AGAMOUS-Like15. Plant Cell **21:** 2563–2577.

Zhou, Q., Hare, P.D., Yang, S.W., Zeidler, M., Huang, L.F., and Chua, N.H. (2005). FHL is required for full phytochrome A signaling and shares overlapping functions with FHY1. Plant J. **43:** 356–370.